

TOWARDS FEDERATED LEARNING ON TIME-EVOLVING HETEROGENEOUS DATA

YongXin Guo*

CUHK (SZ), P.R. China

yongxinguo@link.cuhk.edu.cn

Tao Lin*

EPFL, Switzerland

tao.lin@epfl.ch

Xiaoying Tang

CUHK (SZ), P.R. China

xiaoyingtang@link.cuhk.edu.cn

ABSTRACT

Federated Learning (FL) is an emerging learning paradigm that preserves privacy by ensuring client data locality on edge devices. The optimization of FL is challenging in practice due to the diversity and heterogeneity of the learning system. Despite recent research efforts on improving the optimization of heterogeneous data, the impact of time-evolving heterogeneous data in real-world scenarios, such as changing client data or intermittent clients joining or leaving during training, has not been well studied. In this work, we propose Continual Federated Learning (CFL), a flexible framework, to capture the time-evolving heterogeneity of FL. CFL covers complex and realistic scenarios—which are challenging to evaluate in previous FL formulations—by extracting the information of past local datasets and approximating the local objective functions. Theoretically, we demonstrate that CFL methods achieve a faster convergence rate than FedAvg in time-evolving scenarios, with the benefit being dependent on approximation quality. In a series of experiments, we show that the numerical findings match the convergence analysis, and CFL methods significantly outperform the other SOTA FL baselines.

1 INTRODUCTION

Federated Learning (FL) has recently emerged as a critical distributed machine learning paradigm to preserve user/client privacy. Clients engaged in the training process of FL only communicate their local model parameters, rather than their private local data, with the central server.

As the workhorse algorithm in FL, FedAvg (McMahan et al., 2017) performs multiple local stochastic gradient descent (SGD) updates on the available clients before communicating with the server. Despite its success, FedAvg suffers from the large heterogeneity (non-iid-ness) in the data presented on the different clients, causing drift in each client’s updates and resulting in slow and unstable convergence (Karimireddy et al., 2020b). To address this issue, a new line of study has been suggested lately that either simulates the distribution of the whole dataset using preassigned weights of clients (Wang et al., 2020; Reisizadeh et al., 2020; Mohri et al., 2019; Li et al., 2020a) or adopts variance reduction methods (Karimireddy et al., 2020b;a; Das et al., 2020; Haddadpour et al., 2021). However, the FL formulation in these approaches always assumes a fixed data distribution among clients throughout all training rounds, while in practice this assumption does not always hold because of the complex, uncontrolled, and unpredictable client behaviors. Local datasets, for example, often vary over time, and intermittent clients can join or depart during training without prior notice. The difficulty in addressing the time-evolving heterogeneity of FL lies in the stateless nature of the local datasets, which includes the unpredictable future datasets and the impossibility of retaining all prior local datasets. To this end, we first provide a novel Continual Federated Learning (CFL) formulation and then propose a unified CFL framework as our solution. This framework encompasses a variety of design choices for approximating the local objective functions in the previous training rounds, with the difference between actual and estimated local object functions described as *information loss* for further analysis.

*Equal contribution.

To capture the time-evolving data heterogeneity in the CFL framework, we expand the theoretical assumption on the client drift—which has been extensively utilized recently in Karimireddy et al. (2020b); Khaled et al. (2020); Li et al. (2020b)—to include both client drift and *time drift*. This allows us to quantify the difference between local client objective function and global objective function for the considered time-evolving heterogeneous clients.

We provide convergence rates for our unified CFL framework in conjunction with information loss and new models of both client and time drifts. Our analysis reveals a faster convergence of CFL framework than FedAvg (under time-evolving scenario), with the benefit dependent on approximation accuracy. The rate of CFL can simply recover the rate of FedAvg (under traditional FL scenario) and Continual Learning: the rates of FedAvg obtained from our framework is consistent with previous work, while a similarly simplified rate on Continual Learning (CL) (French, 1999; Kirkpatrick et al., 2017) for the convex and strongly convex cases is novel. Finally, in extensive empirical results, we demonstrate that CFL methods—stemmed from the CFL framework with different approximation techniques—significantly outperform the SOTA FL competitors on various realistic datasets for cross-device and cross-silo FL settings with time-evolving heterogeneous data, including Fashion-MNIST, Cifar10, and Cifar100. These numerical observations corroborate our theoretical findings.

Contribution.

- We present a unified framework, termed Continual Federated Learning (CFL), together with a novel client and time drift modeling approach, to capture complex FL scenarios involving time-evolving heterogeneous data, including standard cross-device FL scenario, stateless scenario, and local dataset overlapping. This is the first theoretical study, to our knowledge, that describes the time-evolving nature of FL.
- We provide rigorous convergence analysis for the CFL methods. Our theoretical analysis explains the faster and more stabilized optimization of the CFL methods over that of FedAvg under time-evolving scenarios, and conjecture their variance reduction effect. In addition, we provide tight convergence rates for standalone CL methods on convex and strongly-convex problems: to the best of our knowledge, we are the first to provide such guarantees for CL on SGD.
- We thoroughly examining some conventional CL methods under the scope of CFL framework: the insights therein offer a valuable practical guideline. We believe filling such gaps is valuable to the FL community and has not been done yet. We demonstrate the efficacy and necessity of CFL methods over the SOTA FL baselines across a range of time-evolving heterogeneous data scenarios and datasets.

2 RELATED WORK

Federated Learning. FedAvg (McMahan et al., 2017; Lin et al., 2020b) is the de facto standard FL algorithm, in which multiple local SGD steps are executed on the available clients to alleviate the communication bottleneck. While communication efficient, heterogeneity, such as system heterogeneity (Li et al., 2018; Wang et al., 2020; Mitra et al., 2021; Diao et al., 2021) and statistical/objective heterogeneity (Li et al., 2018; Wang et al., 2020; Mitra et al., 2021; Lin et al., 2020a; Karimireddy et al., 2020b;a), results in inconsistent optimization objectives and drifted clients models, impeding federated optimization considerably.

A line of work has been proposed to address the heterogeneity in FL. FedProx (Li et al., 2018) adds the regularization term on the distance of local and global models when performing local training—similar formulations can be found in other recent FL works (Hanzely & Richtárik, 2020; Dinh et al., 2020; Li et al., 2021) for various purposes. To address the issue of objective heterogeneity e.g. caused by heterogeneous data, works like SCAFFOLD (Karimireddy et al., 2020b; Mitra et al., 2021) introduce the idea of variance reduction on the client local update steps. FedNova (Wang et al., 2020) further proposes a general framework for unifying FedAvg and FedProx, and argues that while averaging, local updates should be normalized to minimize heterogeneity induced by different number of local update steps. However, most of these prior works focus on the fixed heterogeneity across clients and throughout the entire optimization procedure; we instead consider the novel scenario with time-evolving data heterogeneity.

The theoretical study on the convergence of FedAvg can date back to the parallel SGD analysis on the identical functions Zinkevich et al. (2010) and recently is improved by Stich (2019); Stich & Karimireddy (2020); Patel & Dieuleveut (2019); Khaled et al. (2020); Woodworth et al. (2020b). For the analysis of heterogeneous data, Li et al. (2020b) first give the convergence rate of FedAvg on non-iid datasets with random selection, assuming that the client optimum are ϵ -close. Woodworth et al. (2020a); Khaled et al. (2020) give tighter convergence rates under the assumption of bounded

gradient drift. All above works give a $\mathcal{O}(1/T)$ convergence rate for convex local objective functions. More recently, Karimireddy et al. (2020b); Koloskova et al. (2020) give the convergence analysis of local SGD for non-convex objective functions under bounded gradient noise assumptions, and obtain a $\mathcal{O}(1/\sqrt{T})$ convergence rate. Our theoretical analysis framework covers more challenging time-evolving data heterogeneity in FL, which has not been considered in the community yet—our rate can be simplified to the standard FL scenario, matching the tight analysis in Karimireddy et al. (2020b).

Continual Learning. Continual learning, also known as incremental learning or lifelong learning, aims to learn from (time-evolving) sequential data while avoiding the problem of *catastrophic forgetting* (French, 1999; Kirkpatrick et al., 2017). There exists a large amount of works, from the perspectives of regularization (Kirkpatrick et al., 2017; Li & Hoiem, 2017; Zenke et al., 2017), experience replay (Castro et al., 2018; Rebuffi et al., 2017), and dynamic architectures (Maltoni & Lomonaco, 2019; Rusu et al., 2016). In this paper, we examine both regularization and experience replay based methods, and compare their empirical performance in depth.

Despite the empirical success, the theoretical analysis of CL is limited: only a recent preprint (Yin et al., 2020b) provides a viewpoint of regularization-based continual learning, and only for the single worker scenario. In this work, we provide tight convergence analysis for both CL and CFL on SGD.

Continual Federated Learning. To our knowledge, the scenario of CFL was originally described in Bui et al. (2018) in order to federated train Bayesian Neural Network and continually learn for Gaussian Process models—it is orthogonal to our optimization aspect in this paper. FedCurv (Shoham et al., 2019) blends EWC (Kirkpatrick et al., 2017) regularization with FedAvg, and empirically shows a faster convergence. FedWeIT (Yoon et al., 2021) extends the regularization idea, with a focus on selective inter-client knowledge transfer for task-adaptive parameters. In a very recent parallel (and empirical) work, CDA-FedAvg (Casado et al., 2021) uses a locally maintained long-term data samples, with asynchronous communication. FLwF-2T (?) uses a distillation-based method but still concentrates on class incremental scenarios. Our theoretically sound CFL framework covers the regularization component of FedCurv and the core set part of CDA-FedAvg, and is orthogonal to the neural architecture manipulation idea in FedWeIT.

3 CONTINUAL FEDERATED LEARNING FRAMEWORK

3.1 FORMULATION

Conventional FL Formulation. The standard FL typically considers a sum-structured distributed optimization problem as below:

$$f^* = \min_{\omega \in \mathbb{R}^d} \left[f(\omega) := \sum_{i=1}^N p_i f_i(\omega) \right], \quad (1)$$

where the objective function $f(\omega) : \mathbb{R}^d \rightarrow \mathbb{R}$ is the weighted sum of the local objective functions $f_i(\omega) := \mathbb{E}_{\mathcal{D}_i} [F_i(\omega)]$ of N nodes/clients, and p_i is the weight of client i .

In practice, it may be infeasible to select all clients each round, especially for cross-device setup (McMahan et al., 2017; Kairouz et al., 2019). The standard FedAvg then randomly selects S clients to receive the model parameters from the server ($S \leq N$) in each communication round and performs K local SGD update steps in the form of $\omega_{t,i,k} = \omega_{t,i,k-1} - \eta_l (\nabla f_i(\omega_{t,i,k-1}) + \nu_{t,i,k-1})$, with local step-size η_l and gradient noise $\nu_{t,i,k-1}$. The selected clients then communicate the updates $\Delta\omega_{t,i} = \omega_{t,i,K} - \omega_t$ with the server for the model aggregation: $\omega_{t+1} = \omega_t - \frac{\eta_g}{S} \sum_{i=1}^S \Delta\omega_{t,i}$.

Continual FL Formulation. Despite its wide usage, the standard FL formulation given in Equation (1) cannot properly reflect actual time-evolving scenarios, such as local datasets changing over time or intermittent clients joining or leaving during training. To address this problem, we propose the Continual Federated Learning (CFL) formulation:

$$f^* = \min_{\omega \in \mathbb{R}^d} \left[f(\omega) := \sum_{t=1}^T \sum_{i \in \mathcal{S}_t} p_{t,i} f_{t,i}(\omega) \right], \quad (\text{CFL})$$

where $f_{t,i}(\omega)$ represents the local objective function of client i at time t . \mathcal{S}_t is a subset of clients sampled from all clients set Ω , where $|\mathcal{S}_t| = S$. For the time-evolving scenarios, client i could have different APPROXIMATION FUNCTIONS $f_{t,i}(\omega)$ due to the changing local datasets on different t .

The challenge of addressing (CFL) formulation stems from the stateless nature of the local datasets, which include unpredictable future datasets, as well as the difficulty of keeping all the previous local

Algorithm 1 Approximated CFL Framework

Require: initial weights ω_0 , global learning rate η_g , local learning rate η_l , number of training rounds T
Ensure: trained weights ω_T

```

1: for round  $t = 1, \dots, T$  do
2:   communicate  $\omega_t$  to the chosen clients.
3:   for client  $i \in \mathcal{S}_t$  in parallel do
4:     initialize local model  $\omega_{t,i,0} = \omega_t$ .
5:     for  $k = 1, \dots, K$  do
6:       Calculate stochastic gradient  $\tilde{g}_{t,i,k}$  by (2)
7:        $\omega_{t,i,k} \leftarrow \omega_{t,i,k-1} - \eta_l \tilde{g}_{t,i,k}$ .
8:       communicate  $\Delta\omega_{t,i} \leftarrow \omega_{t,i,K} - \omega_t$ .
9:      $\Delta\omega_t \leftarrow \frac{\eta_g}{S} \sum_{i \in \mathcal{S}_t} \Delta\omega_{t,i}$ .
10:     $\omega_{t+1} \leftarrow \omega_t + \Delta\omega_t$ .

```

datasets. The original definition of (CFL) is theoretically and empirically infeasible. To handle the second case (while ignoring the intractable former), a straightforward approach is to approximate the prior local objective functions (Kirkpatrick et al., 2017; Zenke et al., 2017; Li & Hoiem, 2017), which may be accomplished by retraining information from earlier rounds in accordance with privacy protection standards. Thus, we can express the approximated CFL formulation as:

$$\tilde{f}_t^* = \min_{\omega \in \mathbb{R}^d} \left[\sum_{i \in \mathcal{S}_t} p_{t,i} f_{t,i}(\omega) + \sum_{\tau=1}^{t-1} \sum_{i \in \mathcal{S}_t} p_{\tau,i} \tilde{f}_{\tau,i}(\omega) \right], \quad (2)$$

where $\tilde{f}_{t,i}(\omega)$ denotes the approximated local objective function of client i at time t . In practice, different approximation methods can be used to calculate $\tilde{f}_{\tau,i}(\omega)$, and we refer the detailed illustration and discussions of these approximation algorithms in Section 5.1, Section 5.2, and Appendix C.2.2. We give the formal definition of CFL framework in Algorithm 1. CFL methods are a collection of methods that make use of different approximation techniques and are based on Algorithm 1. We retrieve the objective function of Continual Learning (CL) by setting $S = 1$ in (2).

Take note that in most cases, the previous local object functions cannot be properly approximated. Due to the fact that such approximation impairs optimization, we define the information loss below.

Definition 3.1 (Information Loss). *We define the information loss as the difference between the approximated local objective function $\tilde{f}_{t,i}(\omega)$ and the real local objective function $f_{t,i}(\omega)$, i.e.*

$$\Delta_{t,i}(\omega) = \nabla f_{t,i}(\omega) - \nabla \tilde{f}_{t,i}(\omega). \quad (3)$$

In practice, we use $\|\Delta_{t,i}(\omega)\|_2$ to measure the information loss of different approximation methods. We show large information loss can impede the convergence theoretically (c.f. Theorem 4.1) and empirically (e.g. Figure 1 in Section 5.2).

3.3 GRADIENT NOISE MODEL

To analyze Equation (2) and Algorithm 1 in-depth, we propose the Gradient Noise Model (Equation (5)) to capture the dynamics of performing SGD with data heterogeneity. We first recap the standard definition of gradient noise in Sammut & Webb (2010); Gower et al. (2019).

Gradient noise in SGD. For objective function $f(\omega)$, the gradient with stochastic noise can be defined as $\nabla f(\omega) = g(\omega) + \nu$, where $g(\omega)$ is the stochastic gradient, and ν is a zero-mean noise.

Client drift in FL. To analyze the impact of data heterogeneity, recent works (Karimireddy et al., 2020b; Khaled et al., 2020; Li et al., 2020b) similarly use the gradient noise to capture the distribution drift between local objective function and global objective function:

$$\nabla f(\omega) = \nabla f_i(\omega) + \delta_i, \quad (4)$$

where δ_i is a zero-mean random variable which measures the gradient noise of client i .

Client drift and time drift in CFL framework. Considering the distribution drift in the dimension of client and time, we further modify the gradient noise model in FL as,

$$\nabla f(\omega) = \nabla f_{t,i}(\omega) + \delta_i + \xi_{t,i}. \quad (5)$$

Here we extend the gradient noise to two terms: δ_i and $\xi_{t,i}$. δ_i is a time independent (of t), zero-mean random variable that measures the drift of client i . The zero-mean $\xi_{t,i}$ measures the drift of client i at time t : We assume a fixed underlying client distribution for each client i , and the time drift is only the additive noise for the given client drift. For each client i , an independent time-drift will be sampled for each time step t and added on top of the fixed client drift to capture the time-evolving nature of the clients' local datasets.

Remark 3.2. *To simplify the study and address the cross-device FL settings, we assume that different $\xi_{t,i}$ are independent. A more complicated change pattern of local data may arise in cross-silo FL scenarios in terms of time-dependent $\xi_{t,i}$, resulting in overlapped local datasets. The formulation of these time-dependent scenarios would need some scenario-specific assumptions, which is beyond the scope of this paper. To narrow the gap, in Section 5.2, we experimentally analyze the performance of CFL approaches with overlapped time-evolving local data, and the findings are consistent with our theoretical analysis.*

3.4 ASSUMPTIONS

To ease the theoretical analysis of (CFL) framework, we use the following widely used assumptions.

Assumption 1 (Smoothness and convexity). *Assume local objective functions $f_{t,i}(\omega)$ are L -smooth and μ -convex, i.e. $\frac{\mu}{2} \|\omega_1 - \omega_2\|^2 \leq f_{t,i}(\omega_1) - f_{t,i}(\omega_2) - \langle \nabla f_{t,i}(\omega_2), \omega_1 - \omega_2 \rangle \leq \frac{L}{2} \|\omega_1 - \omega_2\|^2$.*

A widely used corollary is that if a function $f_{t,i}$ is both L -smooth and μ -convex, then it satisfies $\frac{1}{2L} \|\nabla f_{t,i}(\mathbf{x}) - \nabla f_{t,i}(\mathbf{y})\|^2 \leq f_{t,i}(\mathbf{x}) - f_{t,i}(\mathbf{y}) - \nabla f_{t,i}(\mathbf{x})^T(\mathbf{x} - \mathbf{y})$, and $L \geq \mu$.

Assumption 2 (Bounded noise in stochastic gradient). *Let $g_{t,i,k}(\omega) = \nabla f_{t,i,k}(\omega) + \nu_{t,i,k}$, where $\nu_{t,i,k}$ is the stochastic noise of client i on round t at k -th local update step. We assume that $\mathbb{E}[\nu|\omega] = 0$, and $\mathbb{E}[\|\nu\|^2|\omega] \leq \sigma^2$.*

Assumption 1 and 2 are common assumptions in FL (Karimireddy et al., 2020b; Li et al., 2020b). Considering a relaxed assumption like the bounded noise at optimum in Khaled et al. (2020) will be an interesting future research direction. Besides, we introduce the following assumptions to better characterize the client and time drifts in CFL framework (5).

Assumption 3 (Bounded gradient drift of CFL framework). *Let $f(\omega) = \nabla f_{t,i}(\omega) + \delta_i + \xi_{t,i}$, where δ_i measures client drift and $\xi_{t,i}$ indicates the time drift of $\{t, i\}$. We assume $\mathbb{E}[\delta|\omega] = 0$, $\mathbb{E}[\xi|\omega] = 0$, and thus $\mathbb{E}[\|\delta\|^2|\omega] \leq G^2 + B^2 \mathbb{E}\|\nabla f(\omega)\|^2$ and $\mathbb{E}[\|\xi\|^2|\omega] \leq D^2 + A^2 \mathbb{E}\|\nabla f(\omega)\|^2$.*

Assumption 3 assumes the bounded $\mathbb{E}[\|\delta\|^2|\omega]$ and $\mathbb{E}[\|\xi\|^2|\omega]$ in CFL framework, which is equivalent to the widely used (G, B) gradient drift assumption¹ (Gower et al., 2019; Karimireddy et al., 2020b) on the bounded $\mathbb{E}[\|\nabla f_i(\omega)\|^2]$. We prove this claim in Appendix B.1.

Assumption 4 (Bounded information loss). *We assume the information loss $\Delta_{t,i}(\omega)$ can be bounded by an arbitrary non-negative value R , i.e. $\|\Delta_{t,i}(\omega)\| \leq R$.*

Remark 3.3. *The exact information loss in Assumption 4 may be intractable for some approximation methods. In Lemma B.3 of Appendix B.3, we showcase a tight analysis of information loss for Taylor extension based regularization methods.*

4 THEORETICAL RESULTS

In this section, we analyze the theoretical performance of Algorithm 1 under Assumption 1–4. We prove that CFL methods converges faster than FedAvg, despite that the term (refer to φ_t in Theorem 4.1) induced by information loss concurrently trades off the optimization. Additionally, our results include the FedAvg rate (and match the prior work) and a novel convergence rate for SGD on CL. In Table 1, we summarize the convergence rate of different algorithms². The proof details refer to Appendix B.4 and Appendix B.5.

¹The (G, B) gradient drift: $\mathbb{E}[\|\nabla f_i(\omega)\|^2] \leq G^2 \mathbb{E}[\|\nabla f(\omega)\|^2] + B^2$, where $G^2 \geq 1$ and $B^2 \geq 0$.

²To match the notations of prior works that include all clients in all training rounds, we use the abbreviation N to denote the number of selected clients in each round in this section.

Table 1: **Number of communication rounds required to reach $\varepsilon + \varphi$ accuracy** for μ strongly convex and general convex functions under time-evolving FL scenarios (Assumption 1–4). We can recover the rates in conventional FL setups by setting $D = 0$ and $A = 0$. Note that $\varphi = 0$ in FedAvg. Our convergence rate of FedAvg matches the results in Karimireddy et al. (2020b). Our SGD rate of CL on strongly-convex case is novel. Note that all elaborated results using SGD unless specifically mentioned.

Algorithm	Strongly Convex		General Convex
SGD	$\frac{\sigma^2}{\mu NK\varepsilon} + \frac{1}{\mu}$		$\frac{\sigma^2}{NK\varepsilon^2} + \frac{1}{\varepsilon}$
FedAvg	Li et al. (2020b)	$\frac{\sigma^2}{\mu^2 NK\varepsilon} + \frac{(G^2+D^2)K}{\mu^2\varepsilon}$	-
	Khaled et al. (2020)	$\frac{\sigma^2+G^2+D^2}{\mu NK\varepsilon} + \frac{\sigma+G+D}{\mu\sqrt{\varepsilon}} + \frac{N(A^2+B^2)}{\mu}$	$\frac{\sigma^2+G^2+D^2}{NK\varepsilon^2} + \frac{\sigma+G+D}{\mu\varepsilon^{\frac{3}{2}}} + \frac{N(A^2+B^2)}{\varepsilon}$
	Karimireddy et al. (2020b)	$\frac{\sigma^2}{\mu NK\varepsilon} + \frac{G+D}{\mu\sqrt{\varepsilon}} + \frac{c_{p_B}}{\mu}$	$\frac{\sigma^2}{KN\varepsilon^2} + \frac{G+D}{\varepsilon^{\frac{3}{2}}} + \frac{c_{p_B}(D^2+G^2)}{\varepsilon}$
	Woodworth et al. (2020a)	$\frac{\sqrt{c_{p_B}}}{K\sqrt{\mu\varepsilon}} + \frac{\sigma^2 c_{p_B}}{NK\varepsilon^2} + \frac{G+D}{\mu\sqrt{\varepsilon}} + \frac{\sigma}{\mu\sqrt{K\varepsilon}}$	$\frac{c_{p_B}}{K\varepsilon} + \frac{\sigma^2 c_{p_B}}{NK\varepsilon^2} + \frac{(G+D)c_{p_B}}{\varepsilon^{\frac{3}{2}}} + \frac{\sigma c_{p_B}}{\sqrt{K\varepsilon^{\frac{3}{2}}}}$
	Ours	$\frac{\sigma^2}{\mu NK\varepsilon} + \frac{G^2+D^2}{\mu\varepsilon} + \frac{c_{p_B}}{\mu}$	$\frac{c_{p_B}}{\varepsilon} + \frac{\sigma^2}{NK\varepsilon^2} + \frac{G^2+D^2}{\varepsilon^2}$
CL	Yin et al. (2020b)	$\frac{\mu}{\varepsilon} (\text{GD})$	-
	Ours	$\frac{1+A^2}{\mu} + \frac{\sigma^2}{\mu K\varepsilon} + \frac{c_A}{\mu\varepsilon}$	$\frac{c_{p_B}}{\varepsilon} + \frac{\sigma^2}{K\varepsilon^2} + \frac{c_A}{\varepsilon^2}$
CFL	Ours	$\frac{c_{p_B}}{\mu} + \frac{\sigma^2}{\mu NK\varepsilon} + \frac{c_A+G^2}{\mu\varepsilon}$	$\frac{c_{p_B}}{\varepsilon} + \frac{\sigma^2}{NK\varepsilon^2} + \frac{c_A+G^2}{\varepsilon^2}$

$c_{p_B} = 1 + B^2 + A^2$, $c_A = \frac{D^2 R^2}{R^2 + D^2}$. N is the number of chosen clients in each round, and K is the number of local iterations.

4.1 CONVERGENCE RATE OF CFL METHODS

We start our analysis of Algorithm 1 from the one round progress of CFL methods in the Theorem stated below.

Theorem 4.1 (One round Progress of CFL methods). *When $\{f_{t,i}(\omega)\}$ satisfy Assumption 1–4, and let $\eta = K\eta_g\eta_l$, we have the one round progress of CFL methods as,*

$$f(\omega_t) - f(\omega^*) \leq \underbrace{\frac{1}{\eta} \left(1 - \frac{\mu\eta}{2}\right) \mathbb{E} \|\omega_t - \omega^*\|^2 - \frac{1}{\eta} \mathbb{E} \|\omega_{t+1} - \omega^*\|^2}_{A_1} + \underbrace{c_1\eta + c_2\eta^2}_{A_2} + \varphi_t, \quad (6)$$

where $c_1 = 2c_{p_G} + \frac{\sigma^2}{NK} + 2c_R$, $c_2 = \frac{Lc_{p_G}}{3\eta_g^2} + \frac{Lc_R}{6\eta_g^2 K} + \frac{Lc_R}{3\eta_g^2}$, $c_{p_G} = \frac{1}{N} \sum_{i=1}^N G^2 + D^2 (\sum_{\tau=1}^t p_{\tau,i}^2)$, $c_R = \frac{1}{N} \sum_{i=1}^N (\sum_{\tau=1}^{t-1} p_{\tau,i})^2 R^2$. φ_t satisfy $\varphi_t = \mathcal{O} \left(\frac{1}{N} \sum_{i=1}^N \sum_{\tau=1}^{t-1} p_{\tau,i} R \|\omega_0 - \omega^*\| \right)$. N is the number of chosen clients in each round, and K is the number of local iterations.

Theorem 4.1 shows the one round progress of CFL methods. The A_1 part of (6) indicates the linear convergence rate, while the A_2 part illustrates the worsened convergence induced by gradient noise and information loss. φ_t related to the information loss that causes the drift of the optimum. When the upper limit on information loss R exceeds 0, we cannot reach the exact optimum due to the approximation error: the iterates instead reach the neighborhood of $\epsilon + \varphi$, where $\varphi = \frac{\sum_{t=1}^T q_t \varphi_t}{\sum_{t=1}^T q_t}$ for some sequence q_t . We show in Section 5 that in practice, the approximation methods with small information loss converge much better than methods with larger information loss.

Theorem 4.2 (Convergence rate of CFL methods). *Assume $\{f_{t,i}(\omega)\}$ satisfy Assumption 1–4, the output of Algorithm 1 has expected error smaller than $\epsilon + \varphi$, for $\eta_g = 1$, $\eta_l \leq \frac{\sqrt{3+4(1+B^2+A^2)}-\sqrt{4(1+B^2+A^2)}}{6KL\sqrt{1+B^2+A^2}}$, $p_{\tau,i} = \frac{D^2}{tD^2+(t-1)R^2}$ ($\tau < t$), and $p_{t,i} = \frac{(t-1)R^2+D^2}{tD^2+(t-1)R^2}$ on round t . When $\{f_{t,i}(\omega)\}$ are μ -strongly convex functions, we have,*

$$T = \mathcal{O} \left(\frac{Lc_O}{\mu} + \frac{\sigma^2}{\mu NK\varepsilon} + \frac{1}{\mu\varepsilon} (G^2 + \frac{D^2 R^2}{R^2 + D^2}) \right), \quad (7)$$

and when $\{f_{t,i}(\omega)\}$ are general convex functions ($\mu = 0$), we have

$$T = \mathcal{O} \left(\frac{c_O F}{\epsilon} + \frac{\sigma^2 F}{NK\varepsilon^2} + \frac{F}{\varepsilon^2} (G^2 + \frac{D^2 R^2}{R^2 + D^2}) \right), \quad (8)$$

and when $\{f_{t,i}(\omega)\}$ are non-convex, setting $\eta = K\eta_g\eta_l = \frac{\sqrt{KN}}{\sqrt{TL}}$, when $\frac{1}{T} \sum_{t=1}^T \mathbb{E} \left[\|\nabla f(\omega_t)\|^2 \right]$ reach ϵ we have

$$T = \mathcal{O} \left(\frac{L^2(f_0 - f_*)^2}{NKc_m^2\epsilon^2} + \frac{1}{\epsilon^2} \left(\frac{\sqrt{KN}c_{R1}^2}{L} + \frac{\sigma^2}{\sqrt{NK}} \right)^2 \right), \quad (9)$$

where $c_O = 1 + A^2 + B^2$, $c_{R1} = \frac{R^2}{R^2+D^2}$, c_m is a constant related to A , B and R , and $F = \|\omega_0 - \omega^*\|^2$. N is the number of chosen clients in each round, and K is the number of local iterations. We elaborate the choice of $p_{t,i}$ in Appendix B.4.3.

Remark 4.3. When setting $N = 1$ in Theorem 4.2, we recover the convergence rate of standalone CL methods. To the best of our knowledge, we are the first to provide such theoretical guarantees for SGD: the recent work (Yin et al., 2020a) only gives the convergence rate of GD for regularization based CL methods on general convex case, under the constraint of information loss $R = 0$.

Proposition 4.4. For stateless cross-device FL scenarios (clients only appear once during training), we can derive lower bounds than that of Theorem 4.2. More precisely, by applying Lemma B.2 to the considered stateless scenario, the key variance term $c_{normal} = G^2 + \frac{D^2R^2}{R^2+D^2}$ in Theorem 4.2 becomes $c_{stateless} = \frac{(G^2+D^2)R^2}{G^2+D^2+R^2}$. $c_{stateless}$ is the lower bound of c_{normal} , indicating that CFL methods provide higher performance improvements in stateless FL scenarios.

4.2 CONVERGENCE RATE OF FEDAVG UNDER TIME-EVOLVING SCENARIOS

To show the faster convergence of CFL methods than FedAvg, we provide the convergence rate of FedAvg under time-evolving scenarios and Assumption 1–4. Note that prior works only consider traditional FL scenarios (w/o time-evolving heterogeneous data) for FedAvg, and we offer new rates of FedAvg for such scenarios by setting $p_{t,i} = 1$ in Theorem 4.1.

Theorem 4.5 (Convergence rate of FedAvg under time-evolving scenarios). Assume $\{f_{t,i}(\omega)\}$ satisfy Assumption 1–4, the output of FedAvg has expected error smaller than ϵ , for $\eta_g = 1$ and $\eta_l \leq \frac{\sqrt{3+4(1+B^2+A^2)}-\sqrt{4(1+B^2+A^2)}}{6KL\sqrt{1+B^2+A^2}}$. When $\{f_{t,i}(\omega)\}$ are μ -strongly convex functions, we have,

$$T = \mathcal{O} \left(\frac{Lc_O}{\mu} + \frac{\sigma^2}{\mu NK\epsilon} + \frac{G^2+D^2}{\mu\epsilon} \right), \quad (10)$$

and when $\{f_{t,i}(\omega)\}$ are general convex functions ($\mu = 0$), we have

$$T = \mathcal{O} \left(\frac{c_O F}{\epsilon} + \frac{\sigma^2 F}{NK\epsilon^2} + \frac{(G^2+D^2)F}{\epsilon^2} \right), \quad (11)$$

and when $\{f_{t,i}(\omega)\}$ are non-convex, setting $\eta = K\eta_g\eta_l = \frac{\sqrt{KN}}{\sqrt{TL}}$, when $\frac{1}{T} \sum_{t=1}^T \mathbb{E} \left[\|\nabla f(\omega_t)\|^2 \right]$ reach ϵ we have

$$T = \mathcal{O} \left(\frac{L^2(f_0 - f_*)^2}{NKc_m^2\epsilon^2} + \frac{1}{\epsilon^2} \left(\frac{\sqrt{KN}}{L} + \frac{\sigma^2}{\sqrt{NK}} \right)^2 \right), \quad (12)$$

where $c_O = 1 + A^2 + B^2$, and $F = \|\omega_0 - \omega^*\|^2$. N is the number of chosen clients in each round, and K is the number of local iterations.

Note that in both Theorem 4.2 and Theorem 4.5, we only elaborate dominate terms to clarify the difference. Details please refer to Theorem B.5 and B.6 in Appendix B.6.

Remark 4.6. FedAvg (under time-evolving scenarios) is a special case of CFL methods by setting $p_{t,i} = 1$, as stated in Theorem 4.2 and Theorem 4.5. We show in Appendix B.4 that the rate of FedAvg (under time-evolving scenarios) is equivalent to setting the upper bound of information loss $R \rightarrow \infty$. Similar observations can be found by setting $R \rightarrow \infty$ in $p_{t,i} = \frac{(t-1)R^2+D^2}{tD^2+(t-1)R^2}$ in Theorem 4.2.

Remark 4.7. CFL methods accelerate the convergence by reducing the variance term of FedAvg. For example, the gradient noise term $G^2 + D^2$ of FedAvg for convex functions in Theorem 4.5 can be decreased to $G^2 + \frac{D^2R^2}{R^2+D^2}$ in Theorem 4.2. Similarly, the gradient noise term of non-convex functions can be reduced from 1 to $\frac{R^2}{R^2+D^2}$. The benefits of variance reduction in CFL are dependent on the approximation accuracy R , as stated in Remark 4.6.

5 EXPERIMENTS

In our numerical investigation, we first use the Noisy Quadratic Model—a simple convex model—to verify our theoretical results stated in Section 4. The results (in Appendix C.1) demonstrate that CFL methods converge much faster than baselines like FedAvg and FedProx, with a smoother convergence curve. These findings are corroborate Remark 4.7 about the variance reduction effect of CFL methods. We further provide extensive empirical evaluations below by comparing CFL methods with various strong FL competitors on different realistic datasets. We explore several approximation techniques in CFL methods and shed light on achieving practical efficient federated learning with time-evolving data heterogeneity.

5.1 SETUP

Time-evolving heterogeneous local datasets. We consider federated learn an image classifier using ResNet18 on split-CIFAR10 and split-CIFAR100 datasets, as well as a two layer MLP on the split-Fashion-MNIST dataset. The “split” follows the idea introduced in Yurochkin et al. (2019); Hsu et al. (2019); Reddi et al. (2021), where we leverage the Latent Dirichlet Allocation (LDA) to control the distribution drift with parameter α (see Algorithm 4). Larger α indicates smaller drifts.

Unless specifically mentioned otherwise our studies use the following protocol. All datasets are partitioned to 210 subsets for 7 distinct clients: all clients are selected and trained for 500 communication rounds, and each client randomly samples one of the corresponding 30 subsets for the local training—this challenging time-evolving scenario mimics the realistic client data sampling scheme (from some underlying distributions). Notably, the training strategy used in this section is applicable to all FL baselines and CFL methods, and we assess the model performance using a global test dataset³. We carefully tune the hyper-parameters in all algorithms (details refer to Appendix C.2.1), and report the optimal results (i.e. mean test accuracy across the past 5 best epochs) after repeated trials.

Approximation techniques in CFL methods. Below, we review three representative types of information approximation techniques in CL, and use them to investigate the effect of various types of information loss under the (CFL) formulation. We refer to Appendix C.2.2 for a more comprehensive introduction and discussion.

- **Regularization methods.** Instead of keeping datasets from previous rounds, we keep track the gradients and Hessian matrices of local objective functions, and use Taylor Extension to approximate the local objective functions in previous rounds. Note that the trade-off between Hessian estimation and computational overhead constrains the practical feasible of such approach.
- **Core set methods.** Another simple yet effective treatment in CL lies in the category of Exemplar Replay (Rebuffi et al., 2017; Castro et al., 2018). This method selects and regularly saves previous core-set samples (a.k.a. exemplars), and replays them with the current local datasets.
- **Generative methods.** Maintaining a core set for each client may become impractical when learning scales to millions of clients. To ensure a privacy-preserved federated learning, the generative models (Goodfellow et al., 2014) could be used locally to capture the local data distribution; fresh data samples will be generated on the fly and combined with the current local dataset. For the sake of simplicity, we use Markov Chain Monte Carlo (Nori et al., 2014) in our assessment.

5.2 RESULTS

Comments on different CFL approximation techniques. In Table 2, we examine the performance of several approximation techniques using the split-CIFAR10 dataset. We can conclude that (1) *Core set methods outperform other methods by a significant margin*. The simple choice of “naive core set”, i.e. randomly and uniformly sample data from the local dataset, surpasses the sampling technique described in iCaRL (Rebuffi et al., 2017)⁴ for CL, despite their faster convergence in the initial training phase. (2) *The quality of Hessian estimation matters for regularization based methods*. PyHessian (Yao et al., 2020), as a method to approximate diagonal Hessian matrix, is slightly preferable than Fisher Information Matrix, though the latter one involves less computation. (3) *The performance of generative methods is restricted*, and we hypothesize that the poor quality of generated samples contributes to the constraint.

In the subsequent evaluation, we consider naive core set sampling for CFL-Core-Set method, and use PyHessian for CFL-Regularization. We exclude the results of generative methods, due to the trivial performance gain and significant computational overhead.

³The training loss/accuracy on (CFL) formulation are closely aligned with that of global test data, as shown in Figure 5 of Appendix C.2.3. We here only present the global test results for the common interests in practice.

⁴The algorithmic details of the sampling method in iCaRL refer to Algorithm 3 in Appendix C.2.2.

Table 2: **Top-1 accuracy for different choices of approximation techniques in CFL.** We train ResNet18 on split-CIFAR10 dataset (w/ $\alpha = 0.2$) for 300 communication rounds, and the dataset is partitioned to 300 subsets for 10 different clients. All examined algorithms use FedAvg as the backbone.

Algorithm	Regularization Methods		Core Set Methods			Generative Methods	
	PyHessian	Fisher Information Matrix	Naive (Small Set)	Naive (Large Set)	iCaRL (Small Set)	iCaRL (Large Set)	MCMC
Accuracy	74.15 \pm 0.66	73.70 \pm 0.39	77.84 \pm 0.06	78.90 \pm 0.09	76.97 \pm 0.16	77.09 \pm 0.09	74.18 \pm 0.08

Table 3: **Top-1 accuracy of various CFL methods on diverse datasets** for training ResNet18 with 500 communication rounds. In order to observe a noticeable performance difference on Fashion-MNIST, we use $\alpha = 0.1$ instead. All examined algorithms use FedAvg as the backbone. Both CFL-Regularization and CFL-Regularization-Full are regularization based method, and the difference lies on where the regularization is applied: the full version applies regularization to all layers while the other only considers the top layers. R_r indicates the accuracy of CFL-Regularization, while R_f denotes the accuracy of FedAvg.

Algorithm	Accuracy on Fashion-MNIST (%)	Accuracy on CIFAR10 (%)	Accuracy on CIFAR100 (%)
FedAvg	86.75 \pm 0.14	70.51 \pm 0.19	49.97 \pm 0.19
CFL-Regularization	87.02 \pm 0.21	70.86 \pm 0.31	50.69 \pm 0.06
CFL-Core-Set	88.32 \pm 0.12	81.48 \pm 0.24	53.17 \pm 0.08
CFL-Regularization-Full	77.37 \pm 0.63	33.09 \pm 1.45	14.84 \pm 0.12

Metric	Improvement on Fashion-MNIST (%)	Improvement on CIFAR10 (%)	Improvement on CIFAR100 (%)
Absolute ($R_r - R_f$)	0.27	0.35	0.72
Ratio ($(R_r - R_f)/R_f$)	0.31	0.50	1.44

Understanding various approximated CFL implementations on different datasets. Table 3 experimentally studies the impacts of various information approximation techniques in CFL methods—as discussed in Section 5.1—and compares them with the backbone algorithm of CFL methods, i.e. FedAvg. We have the following consistent findings on different datasets.

1. *The improvement of CFL methods over FedAvg becomes larger for more challenging tasks*, as shown in the bottom of the Table 3 for regularization based methods. This might reflect the fact that the precision of the information approximation is more crucial for complicated tasks. Similarly, we demonstrate in Figure 6 (in Appendix C.2.3) that *CFL methods offer better resistance to time-evolving non-iid data* and the significance of such finding is depending on the task difficulty.
2. *For CFL-Regularization method, applying regularization terms on top layers works better than that on all layers*. This observation matches the recent work on decoupling feature extractor and classifier (Collins et al., 2021; Chen & Chao, 2021; Luo et al., 2021): the bottom layers are more generic across tasks and can serve as a global feature extractor, while the top layers are subject to task-specific information.

We further investigate the connection between the information loss and the learning performance. We examine CFL methods with naive core sets, where the degree of information loss⁵ can be changed by altering the core set size from 20 to 150, with the same random seed and optimizers. Figure 1 depicts that the *performance of models is highly linked to the value of information loss: the lesser the information loss, the higher the performance*.

Superior performance of CFL methods over other strong FL baselines. Alongside the comparison between CFL methods and FedAvg on various datasets (Table 2 and Table 3), in Table 4 we verify the efficacy of CFL methods over other strong FL baselines, on split-CIFAR10 dataset. We also examine MimeLite (Karimireddy et al., 2020a), a method suggested for stateless FL scenarios. Note that we exclude the results illustration for methods like SCAFFOLD (Karimireddy et al., 2020b) and Ditto (Li et al., 2021), due to their infeasibility to be applied in our continual scenarios⁶.

We further relax the difficulty of federated continual learning, from challenging non-overlapping time-evolving heterogeneous data (e.g. in Table 2 and Table 3) to a moderate time-evolving case (i.e. the local data evolves with the overlapping, while the size of local datasets stay unchanged). Table 5 illustrates the performance of FL baselines and CFL methods, under different degrees of overlapping (the construction details refers to Appendix C.2.1): *the improvement of CFL methods is consistent to*

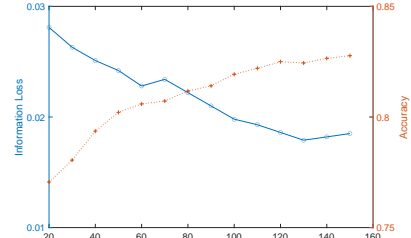


Figure 1: **Information loss** (left y-axis) and **accuracy** (right y-axis) for training ResNet18 on split-CIFAR10 with different core set sizes (x-axis) and $\alpha = 0.2$.

⁵We estimate the information loss by using $\frac{1}{tS} \sum_{i=1}^S \sum_{\tau=1}^t \|\Delta_{\tau,i}(\omega)\|$, where $\Delta_{\tau,i}(\omega)$ is defined in Equation (3), S is the number of clients chosen in each round, and t is the number of communication rounds.

⁶We also naively adapted and examined these methods, but we cannot observe significant performance gains.

Table 4: **Comparing the SOTA FL baselines with several CFL methods**, for training ResNet18 on split-CIFAR10 dataset with different degrees of non-iid-ness α (and with total 500 communication rounds).

Accuracy	FL baselines			CFL methods		
	FedAvg	FedProx	MimeLite	CFL-Core-Set	CFL-Regularization	CFL-Regularization + FedProx
$\alpha = 0.1$	70.51 ± 0.19	71.57 ± 0.17	69.55 ± 0.36	81.48 ± 0.24	70.86 ± 0.31	71.50 ± 0.07
$\alpha = 0.2$	77.98 ± 0.36	78.40 ± 0.22	78.65 ± 0.26	84.41 ± 0.11	78.76 ± 0.26	79.04 ± 0.01

Table 5: **Benchmarking FL baselines and CFL methods on different degrees of local dataset overlapping**, for training ResNet18 on split-CIFAR10 dataset. The overlap reduces the degree of non-iid-ness. In order to observe a noticeable performance difference, we use a larger data distribution gap between rounds (i.e. $\alpha = 0.1$).

Overlap	FL baselines			CFL methods	
	FedAvg	MimeLite	CFL-Core-Set	CFL-Regularization	
0%	80.66 ± 0.40	80.78 ± 0.07	84.87 ± 0.11	81.27 ± 0.38	
25%	80.16 ± 0.01	80.17 ± 0.11	84.66 ± 0.11	80.67 ± 0.27	
50%	79.97 ± 0.23	80.35 ± 0.39	84.59 ± 0.07	80.91 ± 0.25	

Table 6: **Learning with stateless clients**, regarding training ResNet18 on split-CIFAR10 with $\alpha = 0.2$. All examined algorithms use FedAvg as the backbone. The details w.r.t. CFL-Regularization refer to Appendix C.2.2.

Algorithm	FL baselines			CFL methods	
	FedAvg	MimeLite	FedProx	CFL-Regularization	CFL-Regularization + FedProx
Accuracy	78.07 ± 0.06	78.47 ± 0.19	78.48 ± 0.05	79.07 ± 0.25	79.32 ± 0.07

our previous results, while the overlap parameter has no obvious connection with the final global test performance. We believe that both the overlap degree and the new arriving data influence final performance, and we leave future work on realistic time-evolving FL datasets to gain a better understanding.

Investigating stateless FL scenario. In previous numerical investigations, we examine the *stateful clients* and assume that these clients would learn and retain their client states throughout the training process. The remainder of this section will discuss learning with *stateless clients* (i.e. each client only appear once). To do this, we change the data partition strategy such that fresh data partitions are sampled on the fly for each client and communication round.

Table 6 evaluates the above-mentioned scenario. We find that *CFL-Regularization methods consistently outperform alternative FL baselines*, similar to the observations in Table 4. However, due to the nature of stateless under the privacy concern, the advancements of core set method in CFL algorithm cannot be seen in this scenario. Additionally, we discuss the applicability of different algorithms in a variety of time-evolving scenarios in Table 8 of Appendix C.2.3.

REFERENCES

Thang D Bui, Cuong V Nguyen, Siddharth Swaroop, and Richard E Turner. Partitioned variational inference: A unified framework encompassing federated and continual learning. *arXiv preprint arXiv:1811.11206*, 2018.

Fernando E. Casado, Dylan Lema, Marcos F. Criado, Roberto Iglesias, Carlos V. Regueiro, and Senén Barro. Concept drift detection and adaptation for federated and continual learning. *CoRR*, abs/2105.13309, 2021. URL <https://arxiv.org/abs/2105.13309>.

Francisco M Castro, Manuel J Marín-Jiménez, Nicolás Guil, Cordelia Schmid, and Karteek Alahari. End-to-end incremental learning. In *Proceedings of the European conference on computer vision (ECCV)*, pp. 233–248, 2018.

Hong-You Chen and Wei-Lun Chao. On bridging generic and personalized federated learning. *arXiv preprint arXiv:2107.00778*, 2021.

Liam Collins, Hamed Hassani, Aryan Mokhtari, and Sanjay Shakkottai. Exploiting shared representations for personalized federated learning. In *arXiv preprint arXiv:2102.07078*, 2021.

Rudrajit Das, Anish Acharya, Abolfazl Hashemi, Sujay Sanghavi, Inderjit S Dhillon, and Ufuk Topcu. Faster non-convex federated learning via global and local momentum. *arXiv preprint arXiv:2012.04061*, 2020.

Enmao Diao, Jie Ding, and Vahid Tarokh. Heterofl: Computation and communication efficient federated learning for heterogeneous clients. In *International Conference on Learning Representations*, 2021. URL <https://openreview.net/forum?id=TNkPBBYFkXg>.

Canh T Dinh, Nguyen H Tran, and Tuan Dung Nguyen. Personalized federated learning with moreau envelopes. In *Advances in Neural Information Processing Systems*, 2020.

Robert M French. Catastrophic forgetting in connectionist networks. *Trends in cognitive sciences*, 3 (4):128–135, 1999.

Ian J. Goodfellow, Jean Pouget-Abadie, Mehdi Mirza, Bing Xu, David Warde-Farley, Sherjil Ozair, Aaron Courville, and Yoshua Bengio. Generative adversarial networks, 2014.

Robert Mansel Gower, Nicolas Loizou, Xun Qian, Alibek Sailanbayev, Egor Shulgin, and Peter Richtárik. Sgd: General analysis and improved rates. In *International Conference on Machine Learning*, pp. 5200–5209. PMLR, 2019.

Farzin Haddadpour, Mohammad Mahdi Kamani, Aryan Mokhtari, and Mehrdad Mahdavi. Federated learning with compression: Unified analysis and sharp guarantees. In *International Conference on Artificial Intelligence and Statistics*, pp. 2350–2358. PMLR, 2021.

Filip Hanzely and Peter Richtárik. Federated learning of a mixture of global and local models. *arXiv preprint arXiv:2002.05516*, 2020.

Tzu-Ming Harry Hsu, Hang Qi, and Matthew Brown. Measuring the effects of non-identical data distribution for federated visual classification. *arXiv preprint arXiv:1909.06335*, 2019.

Peter Kairouz, H Brendan McMahan, Brendan Avent, Aurélien Bellet, Mehdi Bennis, Arjun Nitin Bhagoji, Kallista Bonawitz, Zachary Charles, Graham Cormode, Rachel Cummings, et al. Advances and open problems in federated learning. *arXiv preprint arXiv:1912.04977*, 2019.

Sai Praneeth Karimireddy, Martin Jaggi, Satyen Kale, Mehryar Mohri, Sashank J Reddi, Sebastian U Stich, and Ananda Theertha Suresh. Mime: Mimicking centralized stochastic algorithms in federated learning. *arXiv preprint arXiv:2008.03606*, 2020a.

Sai Praneeth Karimireddy, Satyen Kale, Mehryar Mohri, Sashank Reddi, Sebastian Stich, and Ananda Theertha Suresh. Scaffold: Stochastic controlled averaging for federated learning. In *International Conference on Machine Learning*, pp. 5132–5143. PMLR, 2020b.

Ahmed Khaled, Konstantin Mishchenko, and Peter Richtárik. Tighter theory for local sgd on identical and heterogeneous data. In *International Conference on Artificial Intelligence and Statistics*, pp. 4519–4529. PMLR, 2020.

James Kirkpatrick, Razvan Pascanu, Neil Rabinowitz, Joel Veness, Guillaume Desjardins, Andrei A Rusu, Kieran Milan, John Quan, Tiago Ramalho, Agnieszka Grabska-Barwinska, et al. Overcoming catastrophic forgetting in neural networks. *Proceedings of the national academy of sciences*, 114 (13):3521–3526, 2017.

Anastasia Koloskova, Nicolas Loizou, Sadra Boreiri, Martin Jaggi, and Sebastian Stich. A unified theory of decentralized sgd with changing topology and local updates. In *International Conference on Machine Learning*, pp. 5381–5393. PMLR, 2020.

Tian Li, Anit Kumar Sahu, Manzil Zaheer, Maziar Sanjabi, Ameet Talwalkar, and Virginia Smith. Federated optimization in heterogeneous networks. *arXiv preprint arXiv:1812.06127*, 2018.

Tian Li, Maziar Sanjabi, Ahmad Beirami, and Virginia Smith. Fair resource allocation in federated learning. In *8th International Conference on Learning Representations, ICLR 2020, Addis Ababa, Ethiopia, April 26-30, 2020*. OpenReview.net, 2020a. URL <https://openreview.net/forum?id=ByexElSYDr>.

Tian Li, Shengyuan Hu, Ahmad Beirami, and Virginia Smith. Ditto: Fair and robust federated learning through personalization. In *International Conference on Machine Learning*, pp. 6357–6368. PMLR, 2021.

Xiang Li, Kaixuan Huang, Wenhao Yang, Shusen Wang, and Zhihua Zhang. On the convergence of fedavg on non-iid data. In *International Conference on Learning Representations*, 2020b. URL <https://openreview.net/forum?id=HJxNAnVtDS>.

Zhizhong Li and Derek Hoiem. Learning without forgetting. *IEEE transactions on pattern analysis and machine intelligence*, 40(12):2935–2947, 2017.

Tao Lin, Lingjing Kong, Sebastian U Stich, and Martin Jaggi. Ensemble distillation for robust model fusion in federated learning. In *Advances in Neural Information Processing Systems*, 2020a.

Tao Lin, Sebastian U. Stich, Kumar Kshitij Patel, and Martin Jaggi. Don’t use large mini-batches, use local sgd. In *International Conference on Learning Representations*, 2020b. URL <https://openreview.net/forum?id=Bley01BFPr>.

Mi Luo, Fei Chen, Dapeng Hu, Yifan Zhang, Jian Liang, and Jiashi Feng. No fear of heterogeneity: Classifier calibration for federated learning with non-iid data. *arXiv preprint arXiv:2106.05001*, 2021.

Davide Maltoni and Vincenzo Lomonaco. Continuous learning in single-incremental-task scenarios. *Neural Networks*, 116:56–73, 2019.

Brendan McMahan, Eider Moore, Daniel Ramage, Seth Hampson, and Blaise Aguera y Arcas. Communication-efficient learning of deep networks from decentralized data. In *Artificial Intelligence and Statistics*, pp. 1273–1282. PMLR, 2017.

Aritra Mitra, Rayana Jaafar, George J Pappas, and Hamed Hassani. Achieving linear convergence in federated learning under objective and systems heterogeneity. *arXiv preprint arXiv:2102.07053*, 2021.

Mehryar Mohri, Gary Sivek, and Ananda Theertha Suresh. Agnostic federated learning. In Kamalika Chaudhuri and Ruslan Salakhutdinov (eds.), *Proceedings of the 36th International Conference on Machine Learning, ICML 2019, 9-15 June 2019, Long Beach, California, USA*, volume 97 of *Proceedings of Machine Learning Research*, pp. 4615–4625. PMLR, 2019. URL <http://proceedings.mlr.press/v97/mohri19a.html>.

Aditya Nori, Chung-Kil Hur, Sriram Rajamani, and Selva Samuel. R2: An efficient mcmc sampler for probabilistic programs. In *Proceedings of the AAAI Conference on Artificial Intelligence*, volume 28, 2014.

Kumar Kshitij Patel and Aymeric Dieuleveut. Communication trade-offs for synchronized distributed sgd with large step size. In *Advances in Neural Information Processing Systems*, 2019.

Sylvestre-Alvise Rebuffi, Alexander Kolesnikov, Georg Sperl, and Christoph H Lampert. icarl: Incremental classifier and representation learning. In *Proceedings of the IEEE conference on Computer Vision and Pattern Recognition*, pp. 2001–2010, 2017.

Sashank J. Reddi, Zachary Charles, Manzil Zaheer, Zachary Garrett, Keith Rush, Jakub Konečný, Sanjiv Kumar, and Hugh Brendan McMahan. Adaptive federated optimization. In *International Conference on Learning Representations*, 2021. URL <https://openreview.net/forum?id=LkFG31B13U5>.

Amirhossein Reisizadeh, Farzan Farnia, Ramtin Pedarsani, and Ali Jadbabaie. Robust federated learning: The case of affine distribution shifts. In Hugo Larochelle, Marc’Aurelio Ranzato, Raia Hadsell, Maria-Florina Balcan, and Hsuan-Tien Lin (eds.), *Advances in Neural Information Processing Systems 33: Annual Conference on Neural Information Processing Systems 2020, NeurIPS 2020, December 6-12, 2020, virtual*, 2020. URL <https://proceedings.neurips.cc/paper/2020/hash/f5e536083a438ce5b64a4954abc17f1-Abstract.html>.

Andrei A Rusu, Neil C Rabinowitz, Guillaume Desjardins, Hubert Soyer, James Kirkpatrick, Koray Kavukcuoglu, Razvan Pascanu, and Raia Hadsell. Progressive neural networks. *arXiv preprint arXiv:1606.04671*, 2016.

Claude Sammut and Geoffrey I. Webb (eds.). *Neuro-Dynamic Programming*, pp. 716–716. Springer US, Boston, MA, 2010. ISBN 978-0-387-30164-8. doi: 10.1007/978-0-387-30164-8_588. URL https://doi.org/10.1007/978-0-387-30164-8_588.

Neta Shoham, Tomer Avidor, Aviv Keren, Nadav Israel, Daniel Benditkis, Liron Mor-Yosef, and Itai Zeitak. Overcoming forgetting in federated learning on non-iid data. *CoRR*, abs/1910.07796, 2019. URL <http://arxiv.org/abs/1910.07796>.

Sebastian U. Stich. Local SGD converges fast and communicates little. In *International Conference on Learning Representations*, 2019. URL <https://openreview.net/forum?id=S1g2JnRcFX>.

Sebastian U Stich and Sai Praneeth Karimireddy. The error-feedback framework: Better rates for sgd with delayed gradients and compressed updates. *Journal of Machine Learning Research*, 21:1–36, 2020.

Jianyu Wang, Qinghua Liu, Hao Liang, Gauri Joshi, and H Vincent Poor. Tackling the objective inconsistency problem in heterogeneous federated optimization. *arXiv preprint arXiv:2007.07481*, 2020.

Blake Woodworth, Kumar Kshitij Patel, and Nathan Srebro. Minibatch vs local sgd for heterogeneous distributed learning. In *NeurIPS 2020 - Thirty-fourth Conference on Neural Information Processing Systems*, 2020a.

Blake Woodworth, Kumar Kshitij Patel, Sebastian Stich, Zhen Dai, Brian Bullins, Brendan McMahan, Ohad Shamir, and Nathan Srebro. Is local sgd better than minibatch sgd? In *International Conference on Machine Learning*, pp. 10334–10343. PMLR, 2020b.

Zhewei Yao, Amir Gholami, Kurt Keutzer, and Michael W. Mahoney. Pyhessian: Neural networks through the lens of the hessian. In Xintao Wu, Chris Jermaine, Li Xiong, Xiaohua Hu, Olivera Kotevska, Siyuan Lu, Weija Xu, Srinivas Aluru, Chengxiang Zhai, Eyhab Al-Masri, Zhiyuan Chen, and Jeff Saltz (eds.), *IEEE International Conference on Big Data, Big Data 2020, Atlanta, GA, USA, December 10-13, 2020*, pp. 581–590. IEEE, 2020. doi: 10.1109/BigData50022.2020.9378171. URL <https://doi.org/10.1109/BigData50022.2020.9378171>.

Dong Yin, Mehrdad Farajtabar, and Ang Li. SOLA: continual learning with second-order loss approximation. *CoRR*, abs/2006.10974, 2020a. URL <https://arxiv.org/abs/2006.10974>.

Dong Yin, Mehrdad Farajtabar, Ang Li, Nir Levine, and Alex Mott. Optimization and generalization of regularization-based continual learning: a loss approximation viewpoint. *arXiv preprint arXiv:2006.10974*, 2020b.

Jaehong Yoon, Wonyong Jeong, Giwoong Lee, Eunho Yang, and Sung Ju Hwang. Federated continual learning with weighted inter-client transfer. In *International Conference on Machine Learning*, pp. 12073–12086. PMLR, 2021.

Mikhail Yurochkin, Mayank Agarwal, Soumya Ghosh, Kristjan Greenewald, Nghia Hoang, and Yasaman Khazaeni. Bayesian nonparametric federated learning of neural networks. In *International Conference on Machine Learning*, pp. 7252–7261. PMLR, 2019.

Friedemann Zenke, Ben Poole, and Surya Ganguli. Continual learning through synaptic intelligence. In *International Conference on Machine Learning*, pp. 3987–3995. PMLR, 2017.

Guodong Zhang, Lala Li, Zachary Nado, James Martens, Sushant Sachdeva, George E Dahl, Christopher J Shallue, and Roger Grosse. Which algorithmic choices matter at which batch sizes? insights from a noisy quadratic model. In *Advances in Neural Information Processing Systems*, 2019.

Martin Zinkevich, Markus Weimer, Alexander J Smola, and Lihong Li. Parallelized stochastic gradient descent. In *NIPS*, volume 4, pp. 4. Citeseer, 2010.

CONTENTS OF APPENDIX

A Techniques	14
B Convergence rate of CFL	15
B.1 Bound of Gradient Noise	15
B.2 Bounded Gradient Noise of CFL	15
B.3 Bounded Approximation Error	16
B.4 Proof of Theorem 4.2	16
B.4.1 Start up.	16
B.4.2 One Step Progress	17
B.4.3 Weights of rounds.	20
B.4.4 Convergence results	20
B.5 Proof of convergence rate for non-convex setting	22
B.6 Theoretical Results	25
C Experiment details	26
C.1 Noisy quadratic model	26
C.2 Realistic datasets	27
C.2.1 Setup	27
C.2.2 Approximation Methods	28
C.2.3 Additional Experiments	29
C.3 Algorithms	29

A TECHNIQUES

Here we show some technical lemmas which are helpful in the theoretical proof.

Lemma A.1 (Linear convergence rate (Karimireddy et al., 2020b, Lemma 1)). *For every non-negative sequence $\{d_{r-1}\}_{r \geq 1}$, and any parameter $\mu > 0$, $T \geq \frac{1}{2\eta_{max}\mu}$, there exists a constant step-size $\eta \leq \eta_{max}$ and weights $\omega_t = (1 - \mu\eta)^{1-t}$ such that for $W_T = \sum_{t=1}^{T+1} \omega_t$*

$$\Phi_T = \frac{1}{W_T} \sum_{t=1}^{T+1} \left(\frac{\omega_{t-1}}{\eta} (1 - \mu\eta) d_{t-1} - \frac{\omega_t}{\eta} d_t \right) = \tilde{\mathcal{O}}(\mu d_0 \exp(-\mu\eta_{max}T)). \quad (13)$$

Lemma A.2 (Sub-linear convergence rate (Karimireddy et al., 2020b, Lemma 2)). *For every non-negative sequence $\{d_{r-1}\}_{r \geq 1}$ and any parameters $\eta_{max} > 0$, $c_1 \geq 0$, $c_2 \geq 0$, $T \geq 0$, there exists a constant step-size $\eta \leq \eta_{max}$ such that*

$$\Phi_T = \frac{1}{T+1} \sum_{t=1}^{T+1} \left(\frac{d_{t-1}}{\eta} - \frac{d_t}{\eta} + c_1\eta + c_2\eta^2 \right) \leq \frac{d_0}{\eta_{max}(T+1)} + \frac{2\sqrt{c_1 d_0}}{\sqrt{T+1}} + 2 \left(\frac{d_0}{T+1} \right)^{\frac{2}{3}} c_2^{\frac{1}{3}}. \quad (14)$$

Lemma A.3 (Relaxed triangle inequality (Karimireddy et al., 2020b, Lemma 3)). *Let $\{\mathbf{v}_1, \dots, \mathbf{v}_\tau\}$ be τ vectors in \mathcal{R}^d . Then the following is true:*

$$\left\| \frac{1}{\tau} \sum_{i=1}^{\tau} \mathbf{v}_i \right\|^2 \leq \frac{1}{\tau} \sum_{i=1}^{\tau} \|\mathbf{v}_i\|^2. \quad (15)$$

Lemma A.4 (Separating mean and variance (Stich & Karimireddy, 2020, Lemma 14)). *Let $\Xi_1, \Xi_2, \dots, \Xi_\tau$ be τ random variables in \mathcal{R}^d which are not necessarily independent. First suppose that their mean is $E[\Xi_i] = \xi_i$, and variance is bounded as $\mathbb{E}\|\Xi_i - \xi_i\|^2 \leq M\|\xi_i\|^2 + \sigma^2$, then the following holds*

$$\mathbb{E} \left\| \sum_{i=1}^{\tau} \Xi_i \right\|^2 \leq (\tau + M) \sum_{i=1}^{\tau} \|\xi_i\|^2 + \tau\sigma^2. \quad (16)$$

Lemma A.5 (Perturbed strongly convexity (Karimireddy et al., 2020b, Lemma 5)). *The following holds for any L -smooth and μ -strongly convex function h , and any $\mathbf{x}, \mathbf{y}, \mathbf{z}$ in the domain of h :*

$$\langle \nabla h(\mathbf{x}), \mathbf{z} - \mathbf{y} \rangle \geq h(\mathbf{z}) - h(\mathbf{y}) + \frac{\mu}{4} \|\mathbf{y} - \mathbf{z}\|^2 - L\|\mathbf{z} - \mathbf{x}\|^2. \quad (17)$$

Lemma A.6. Define $S = \sum_{t=1}^T \frac{p_t}{t}$ where $\sum_{t=1}^T p_t = 1$, and $p_t \leq p_{t+1}$ then $S \leq \frac{1}{T} \sum_{t=1}^T \frac{1}{t} = \tilde{\mathcal{O}}\left(\frac{\ln T}{T}\right)$.

B CONVERGENCE RATE OF CFL

B.1 BOUND OF GRADIENT NOISE

Lemma B.1 (Bound of Gradient Noise). Suppose $f_i(\omega)$ is the local objective function, and $f(\omega) = \mathbb{E}[f_i(\omega)]$ is the global objective function. Define $\nabla f(\omega) = \nabla f_i(\omega) + \varsigma_i$, $\mathbb{E}[\varsigma_i] = 0$, and assume $\mathbb{E}\left[\|\varsigma\|^2 | \omega\right] \leq A^2 \mathbb{E}\left[\|\nabla f(\omega)\|^2\right] + B^2$, we have

$$\mathbb{E}\left[\|\nabla f_i(\omega)\|^2\right] \leq (A^2 + 1)\mathbb{E}\left[\|\nabla f(\omega)\|^2\right] + B^2. \quad (18)$$

Proof.

$$\mathbb{E}\left[\|\nabla f_i(\omega)\|^2\right] = \mathbb{E}\left[\|\nabla f(\omega) + \varsigma_i\|^2\right] \quad (19)$$

$$= \mathbb{E}\left[\|\nabla f(\omega)\|^2\right] + \mathbb{E}\left[\|\varsigma_i\|^2\right] \quad (20)$$

$$\leq (A + 1)\mathbb{E}\left[\|\nabla f(\omega)\|^2\right] + B. \quad (21)$$

□

B.2 BOUNDED GRADIENT NOISE OF CFL

Lemma B.2 (Bounded Gradient Noise of CFL). For Formulation (CFL), consider CFL and FedAvg, we can bound the gradient drift as

(1) FedAvg only optimize current local objective functions, thus,

$$\mathbb{E}\|\nabla f_{t,i}(\omega)\|^2 \leq (1 + A^2 + B^2)\mathbb{E}\|\nabla f(\omega)\|^2 + G^2 + D^2.$$

(2) For CFL, in general (same clients can appear in different rounds), we have

$$\begin{aligned} \mathbb{E}\left\|\sum_{\tau=1}^t p_{\tau,i} \nabla f_{\tau,i}(\omega)\right\|^2 &\leq \left(1 + B^2 + A^2 \sum_{\tau=1}^t p_{\tau,i}^2\right) \mathbb{E}\|\nabla f(\omega)\|^2 \\ &\quad + G^2 + D^2 \sum_{\tau=1}^t p_{\tau,i}^2. \end{aligned}$$

(3) For CFL, when clients only participate in training once ($\delta_{t,i}$ are independent for all t and i), we have

$$\begin{aligned} \mathbb{E}\left\|\sum_{\tau=1}^t p_{\tau,i} \nabla f_{\tau,i}(\omega)\right\|^2 &\leq \left(1 + (B^2 + A^2) \sum_{\tau=1}^t p_{\tau,i}^2\right) \mathbb{E}\|\nabla f(\omega)\|^2 \\ &\quad + (G^2 + D^2) \sum_{\tau=1}^t p_{\tau,i}^2. \end{aligned}$$

Proof. Using Assumption 3, together with the fact that $\nabla f_{t,i}(\omega) = \nabla f(\omega) + \delta_{t,i} + \xi_{t,i}$ (Here to simplify the notation, we use $\{t, i\}$ pair to denote the client participate in training on round t and number i), we have

$$\mathbb{E}\|\nabla f_{t,i}(\omega)\|^2 = \mathbb{E}\|\nabla f(\omega) + \delta_{t,i} + \xi_{t,i}\|^2 \quad (22)$$

$$= \mathbb{E}\|\nabla f(\omega)\|^2 + \mathbb{E}\|\delta_{t,i}\|^2 + \mathbb{E}\|\xi_{t,i}\|^2 \quad (23)$$

$$\leq (1 + A^2 + B^2)\mathbb{E}\|\nabla f(\omega)\|^2 + G^2 + D^2. \quad (24)$$

The second inequality is based on the independence of noise, and directly use Assumption 3 we get the last inequality. Similarly, we have

$$\mathbb{E} \left\| \sum_{\tau=1}^t p_{\tau,i} \nabla f_{\tau,i}(\boldsymbol{\omega}) \right\|^2 = \mathbb{E} \left\| \sum_{\tau=1}^t p_{\tau,i} (\nabla f_{\tau,i}(\boldsymbol{\omega}) + \boldsymbol{\delta}_i + \boldsymbol{\xi}_{\tau,i}) \right\|^2 \quad (25)$$

$$= \mathbb{E} \|\nabla f(\boldsymbol{\omega})\|^2 + \mathbb{E} \|\boldsymbol{\delta}_i\|^2 + \mathbb{E} \left\| \sum_{\tau=1}^t p_{\tau,i} \boldsymbol{\xi}_{\tau,i} \right\|^2 \quad (26)$$

$$\leq \left(1 + A^2 + B^2 \sum_{\tau=1}^t p_{\tau,i}^2 \right) \mathbb{E} \|\nabla f(\boldsymbol{\omega})\|^2 + G^2 + D^2 \sum_{\tau=1}^t p_{\tau,i}^2. \quad (27)$$

For the last inequality, when $\boldsymbol{\delta}_{t_1,i}$ and $\boldsymbol{\delta}_{t_2,i}$ are independent for all t_1, t_2 ,

$$\mathbb{E} \left\| \sum_{\tau=1}^t p_{\tau,i} \nabla f_{\tau,i}(\boldsymbol{\omega}) \right\|^2 = \mathbb{E} \left\| \sum_{\tau=1}^t p_{\tau,i} (\nabla f_{\tau,i}(\boldsymbol{\omega}) + \boldsymbol{\delta}_{t,i} + \boldsymbol{\xi}_{\tau,i}) \right\|^2 \quad (28)$$

$$= \mathbb{E} \|\nabla f(\boldsymbol{\omega})\|^2 + \mathbb{E} \left\| \sum_{\tau=1}^t p_{\tau,i} \boldsymbol{\delta}_{t,i} \right\|^2 + \mathbb{E} \left\| \sum_{\tau=1}^t p_{\tau,i} \boldsymbol{\xi}_{\tau,i} \right\|^2 \quad (29)$$

$$\leq \left(1 + (A^2 + B^2) \sum_{\tau=1}^t p_{\tau,i}^2 \right) \mathbb{E} \|\nabla f(\boldsymbol{\omega})\|^2 + (G^2 + D^2) \sum_{\tau=1}^t p_{\tau,i}^2. \quad (30)$$

□

B.3 BOUNDED APPROXIMATION ERROR

Lemma B.3 (Bounded Approximation Error). *For $\Delta_{t,i}(\boldsymbol{\omega}) = \nabla f_{t,i}(\boldsymbol{\omega}) - \nabla \tilde{f}_{t,i}(\boldsymbol{\omega})$ (c.f. Definition 3), when use Taylor Extension,*

$$\nabla \tilde{f}_{t,i}(\boldsymbol{\omega}) = \nabla f_{t,i}(\boldsymbol{\omega}_t) + \nabla^2 f_{t,i}(\boldsymbol{\omega}_t)(\boldsymbol{\omega} - \boldsymbol{\omega}_t),$$

we have

$$\|\Delta_{t,i}(\boldsymbol{\omega})\| \leq \epsilon \|\boldsymbol{\omega} - \hat{\boldsymbol{\omega}}_{t,i}\|.$$

Proof.

$$\|\Delta_{t,i}(\boldsymbol{\omega})\| = \|\nabla f_{t,i}(\boldsymbol{\omega}) - \nabla \tilde{f}_{t,i}(\boldsymbol{\omega})\| \quad (31)$$

$$= \|\nabla f_{t,i}(\boldsymbol{\omega}) - \nabla f_{t,i}(\boldsymbol{\omega}_{t,i,K}) - \mathbf{H}_{tjK}(\boldsymbol{\omega} - \boldsymbol{\omega}_{t,i,K})\| \quad (32)$$

$$= \|\nabla^2 f_{t,i}(\boldsymbol{\omega}_{\xi,t})(\boldsymbol{\omega} - \boldsymbol{\omega}_{t,i,K}) - \mathbf{H}_{tjK}(\boldsymbol{\omega} - \boldsymbol{\omega}_{t,i,K})\| \quad (33)$$

$$= \|(\nabla^2 f_{t,i}(\boldsymbol{\omega}_{\xi,t}) - \mathbf{H}_{tjK})(\boldsymbol{\omega} - \boldsymbol{\omega}_{t,i,K})\| \quad (34)$$

$$\leq \epsilon \|\boldsymbol{\omega} - \boldsymbol{\omega}_{t,i,K}\|. \quad (35)$$

The first two equations come from the mean value theorem which says for continuous function f in closed intervals $[a, b]$ and differentiable on open interval (a, b) , there exists a point $c \subseteq (a, b)$ such that

$$f'(c) = \frac{f(b) - f(a)}{b - a}. \quad (36)$$

The last inequality is based on Assumption 4. □

B.4 PROOF OF THEOREM 4.2

In this section we will give the complete proof of convergence rate of algorithm 2 when the local objective functions are convex.

B.4.1 START UP.

The local objective function of round t on client i is

$$\bar{f}_{t,i}(\boldsymbol{\omega}) = (p_{t,i} f_{t,i}(\boldsymbol{\omega}) + \sum_{\tau=1}^{t-1} p_{\tau,i} \tilde{f}_{\tau,i}(\boldsymbol{\omega})). \quad (37)$$

Algorithm 2 CFL Framework

Require: initial weights ω_0 , global learning rate η_g , local learning rate η_l

```

1: for round  $t = 1, \dots, T$  do
2:   communicate  $\omega_t$  to the chosen clients.
3:   for client  $i \in \mathcal{S}_t$  in parallel do
4:     initialize local model  $\omega_{t,i,0} = \omega_t$ .
5:     for  $k = 1, \dots, K$  do
6:        $\tilde{g}_{t,i,k}(\omega_{t,i,k-1}) = \left( p_{t,i} \nabla f_{t,i}(\omega_{t,i,k-1}) + \sum_{\tau=1}^{t-1} p_{\tau,i} \nabla \tilde{f}_{\tau,i}(\omega_{t,i,k-1}) \right) + \nu_{t,i,k}$ .
7:        $\omega_{t,i,k} \leftarrow \omega_{t,i,k-1} - \eta_l \tilde{g}_{t,i,k}(\omega_{t,i,k-1})$ .
8:     communicate  $\Delta\omega_{t,i} \leftarrow \omega_{t,i,K} - \omega_t$ .
9:      $\Delta\omega_t \leftarrow \frac{\eta_g}{S} \sum_{i \in \mathcal{S}_t} \Delta\omega_{t,i}$ .
10:     $\omega_{t+1} \leftarrow \omega_t + \Delta\omega_t$ .

```

Without loss of generality, assume $\sum_{\tau=1}^t p_{\tau,i} = 1$. Then follow the steps in algorithm 2, we have

$$\nabla \bar{f}_{t,i}(\omega) = p_{t,i} \nabla f_{t,i}(\omega) + \sum_{\tau=1}^{t-1} p_{\tau,i} \nabla \tilde{f}_{\tau,i}(\omega). \quad (38)$$

Then the noisy gradient in mini-batch SGD can be described as

$$\bar{g}_{t,i,k}(\omega_{t,i,k-1}) = \nabla \bar{f}_{t,i}(\omega_{t,i,k-1}) + \nu_{t,i,k} \quad (39)$$

Then follow the steps in algorithm 2, we have

$$\Delta\omega_t = \frac{-\eta_l \eta_g}{N} \sum_{i=1}^N \sum_{k=1}^K \bar{g}_{t,i}(\omega_{t,i,k-1}), \quad (40)$$

$$E[\Delta\omega_t] = \frac{-\eta_l \eta_g}{N} \sum_{i=1}^N \sum_{k=1}^K \nabla \bar{f}_{t,i}(\omega_{t,i,k-1}). \quad (41)$$

Then let $\eta = K\eta_l\eta_g$, we have

$$\Delta\omega_t = \frac{-\eta}{NK} \sum_{i=1}^N \sum_{k=1}^K \bar{g}_{t,i}(\omega_{t,i,k-1}), \quad (42)$$

$$E[\Delta\omega_t] = \frac{-\eta}{NK} \sum_{i=1}^N \sum_{k=1}^K \nabla \bar{f}_{t,i}(\omega_{t,i,k-1}). \quad (43)$$

B.4.2 ONE STEP PROGRESS

Consider the one-step progress we have

$$\mathbb{E}\|\omega_t + \Delta\omega_t - \omega^*\|^2 = \|\omega_t - \omega^*\|^2 - \underbrace{2E\langle \omega_t - \omega^*, \Delta\omega_t \rangle}_{A_1} + \underbrace{\mathbb{E}\|\Delta\omega_t\|^2}_{A_2}. \quad (44)$$

Firstly we consider A_1 part in equation (44),

$$\begin{aligned} & -2E\langle \omega_t - \omega^*, \Delta\omega_t \rangle \\ &= \frac{2\eta}{NK} \sum_{i=1}^N \sum_{k=1}^K \langle \nabla \bar{f}_{t,i}(\omega_{t,i,k-1}), \omega^* - \omega_t \rangle \end{aligned} \quad (45)$$

$$= \frac{2\eta}{NK} \sum_{i=1}^N \sum_{k=1}^K \langle p_{t,i} \nabla f_{t,i}(\omega_{t,i,k}) + \sum_{\tau=1}^{t-1} p_{\tau,i} \nabla \tilde{f}_{\tau,i}(\omega_{t,i,k}), \omega^* - \omega_t \rangle \quad (46)$$

$$= \frac{2\eta}{NK} \sum_{i=1}^N \sum_{k=1}^K \sum_{\tau=1}^t \langle p_{\tau,i} \nabla f_{\tau,i}(\omega_{t,i,k}), \omega^* - \omega_t \rangle - \frac{2\eta}{NK} \sum_{i=1}^N \sum_{k=1}^K \sum_{\tau=1}^{t-1} p_{\tau,i} \langle \Delta_{\tau,i}(\omega_{t,i,k}), \omega^* - \omega_t \rangle \quad (47)$$

$$\leq \frac{2\eta}{NK} \sum_{i=1}^N \sum_{k=1}^K \sum_{\tau=1}^t p_{\tau,i} \langle \nabla f_{\tau,i}(\omega_{t,i,k}), \omega^* - \omega_t \rangle + \frac{2\eta}{N} \sum_{i=1}^N \sum_{\tau=1}^{t-1} p_{\tau,i} R \|\omega^* - \omega_t\|. \quad (48)$$

We use equality (43) for first inequality, and directly use Assumption 4 and Cauchy–Schwarz inequality for last inequality.

Then we can consider the first term of inequality (48). Firstly, by Lemma A.5 we see that

$$\langle \nabla f_{\tau,i}(\omega_{t,i,k-1}), \omega^* - \omega_t \rangle \leq f_{\tau,i}(\omega^*) - f_{\tau,i}(\omega_t) - \frac{\mu}{4} \|\omega_t - \omega^*\|^2 + L \|\omega_{t,i,k-1} - \omega_t\|^2. \quad (49)$$

That is, based on (48) and (49), we have,

$$\begin{aligned} & -2E\langle \omega_t - \omega^*, \Delta\omega_t \rangle \\ & \leq -2\eta(f_t(\omega_t) - f_t(\omega^*) + \frac{\mu}{4} \|\omega_t - \omega^*\|^2) + \frac{2\eta L}{NK} \sum_{i=1}^N \sum_{k=1}^K \|\omega_{t,i,k-1} - \omega_t\|^2 \\ & \quad + 2\eta \sum_{\tau=1}^{t-1} p_{\tau,i} R \|\omega^* - \omega_t\|. \end{aligned} \quad (50)$$

Then consider A_2 in (44), and define $c_{p_B,i} = 1 + B^2 + A^2(\sum_{\tau=1}^t p_{\tau,i}^2)$, $c_{p_G,i} = G^2 + D^2(\sum_{\tau=1}^t p_{\tau,i}^2)$, $c_{p_B} = \frac{1}{N} \sum_{i=1}^N c_{p_B,i}$, and $c_{p_G} = \frac{1}{N} \sum_{i=1}^N c_{p_G,i}$ we have

$$\mathbb{E}\|\Delta\omega_t\|^2$$

$$= \frac{\eta^2}{N^2 K^2} \mathbb{E} \left\| \sum_{i=1}^N \sum_{k=1}^K \left(p_{t,i} \nabla f_{t,i}(\omega_{t,i,k-1}) + \sum_{\tau=1}^{t-1} p_{\tau,i} \nabla \tilde{f}_{\tau,i}(\omega_{t,i,k-1}) + \nu_{t,i,k} \right) \right\|^2 \quad (51)$$

$$= \frac{\eta^2}{N^2 K^2} \mathbb{E} \left\| \sum_{i=1}^N \sum_{k=1}^K \left(\sum_{\tau=1}^t p_{\tau,i} \nabla f_{\tau,i}(\omega_{t,i,k-1}) - \sum_{\tau=1}^{t-1} p_{\tau,i} \Delta_{\tau,i}(\omega_{t,i,k-1}) + \nu_{t,i,k} \right) \right\|^2 \quad (52)$$

$$\stackrel{\text{Lem A.4}}{\leq} \frac{\eta^2}{NK} \sum_{i=1}^N \sum_{k=1}^K \mathbb{E} \left\| \sum_{\tau=1}^t p_{\tau,i} \nabla f_{\tau,i}(\omega_{t,i,k-1}) - \sum_{\tau=1}^{t-1} p_{\tau,i} \Delta_{\tau,i}(\omega_{t,i,k-1}) \right\|^2 + \frac{\eta^2 \sigma^2}{NK} \quad (53)$$

$$\stackrel{\text{Lem A.3}}{\leq} \frac{2\eta^2}{NK} \sum_{i=1}^N \sum_{k=1}^K \left(\mathbb{E} \left\| \sum_{\tau=1}^t p_{\tau,i} \nabla f_{\tau,i}(\omega_{t,i,k-1}) \right\|^2 + \mathbb{E} \left\| \sum_{\tau=1}^{t-1} p_{\tau,i} \Delta_{\tau,i}(\omega_{t,i,k-1}) \right\|^2 \right) + \frac{\eta^2 \sigma^2}{NK} \quad (54)$$

$$\stackrel{\text{Lem ??}}{\leq} \frac{2\eta^2}{NK} \sum_{i=1}^N \sum_{k=1}^K \left(\left(1 + B^2 + A^2(\sum_{\tau=1}^t p_{\tau,i}^2) \right) \mathbb{E} \|\nabla f(\omega_{t,i,k-1})\|^2 + \left(G^2 + D^2(\sum_{\tau=1}^t p_{\tau,i}^2) \right) \right) + \frac{2\eta^2}{N} \sum_{i=1}^N (\sum_{\tau=1}^{t-1} p_{\tau,i})^2 R^2 + \frac{\eta^2 \sigma^2}{NK} \quad (55)$$

$$\stackrel{\text{Lem A.3}}{\leq} \frac{4\eta^2}{NK} \sum_{i=1}^N \sum_{k=1}^K c_{p_B,i} (\mathbb{E} \|\nabla f(\omega_{t,i,k-1}) - \nabla f(\omega_t)\|^2 + \mathbb{E} \|\nabla f(\omega_t)\|^2) + 2\eta^2 c_{p_G} + \frac{2\eta^2}{N} \sum_{i=1}^N (\sum_{\tau=1}^{t-1} p_{\tau,i})^2 R^2 + \frac{\eta^2 \sigma^2}{NK} \quad (56)$$

$$\stackrel{\text{Ass } 1}{\leq} 16\eta^2 L c_{p_B} (f(\omega_t) - f(\omega^*)) + \frac{8\eta^2 L^2}{NK} \sum_{i=1}^N \sum_{k=1}^K c_{p_B,i} \mathbb{E} \|\omega_{t,i,k-1} - \omega_t\|^2 + 2\eta^2 c_{p_G} + \frac{2\eta^2}{N} \sum_{i=1}^N (\sum_{\tau=1}^{t-1} p_{\tau,i})^2 R^2 + \frac{\eta^2 \sigma^2}{NK}. \quad (57)$$

Then consider equation (50) and (57), to solve $\mathbb{E}\|\omega_{t,i,k-1} - \omega_t\|^2$, we have

$$\mathbb{E}\|\omega_{t,i,k} - \omega_t\|^2 = \eta_l^2 \mathbb{E} \left\| \sum_{\tau=1}^k \bar{g}_{t,i}(\omega_{t,i,\tau-1}) \right\|^2 \quad (58)$$

$$\stackrel{\text{Lem A.4}}{\leq} k\eta_l^2 \sum_{\tau=1}^k \mathbb{E}\|\nabla \bar{f}_{t,i}(\omega_{t,i,\tau-1})\|^2 + k\eta_l^2\sigma^2. \quad (59)$$

Here we directly use Lemma A.4 to get inequality (59).

Then for $\mathbb{E}\|\nabla \bar{f}_{t,i}(\omega)\|^2$, we have

$$\begin{aligned} & \mathbb{E}\|\nabla \bar{f}_{t,i}(\omega)\|^2 \\ &= \mathbb{E}\left\| p_{t,i} \nabla f_{t,i}(\omega) + \sum_{\tau=1}^{t-1} p_{\tau,i} \nabla \tilde{f}_{\tau,i}(\omega) \right\|^2 \end{aligned} \quad (60)$$

$$= \mathbb{E}\left\| \sum_{\tau=1}^t p_{\tau,i} \nabla f_{\tau,i}(\omega) - \sum_{\tau=1}^{t-1} p_{\tau,i} \Delta_{\tau,i}(\omega) \right\|^2 \quad (61)$$

$$\stackrel{\text{Lem A.3}}{\leq} 2\mathbb{E}\left\| \sum_{\tau=1}^t p_{\tau,i} \nabla f_{\tau,i}(\omega) \right\|^2 + 2\mathbb{E}\left\| \sum_{\tau=1}^{t-1} p_{\tau,i} \Delta_{\tau,i}(\omega) \right\|^2 \quad (62)$$

$$\stackrel{\text{Lem ??}}{\leq} 2c_{p_B,i} \mathbb{E}\|\nabla f(\omega)\|^2 + 2c_{p_G,i} + 2(\sum_{\tau=1}^{t-1} p_{\tau,i})^2 R^2 \quad (63)$$

$$\stackrel{\text{Ass 1}}{\leq} 4L^2 c_{p_B,i} \mathbb{E}\|\omega - \omega_t\|^2 + 8Lc_{p_B,i} (f(\omega_t) - f(\omega^*)) + 2c_{p_G,i} + 2(\sum_{\tau=1}^{t-1} p_{\tau,i})^2 R^2. \quad (64)$$

Combine equation (59) and (64) we get,

$$\begin{aligned} & \mathbb{E}\|\omega_{t,i,k} - \omega_t\|^2 \\ & \leq 4k^2\eta_l^2 L^2 c_{p_B,i} \mathbb{E}\|\omega_{t,i,k-1} - \omega_t\|^2 + 8k^2\eta_l^2 L c_{p_B,i} (f(\omega_t) - f(\omega^*)) + 2k^2\eta_l^2 c_{p_G,i} + 2k^2\eta_l^2 (\sum_{\tau=1}^{t-1} p_{\tau,i})^2 R^2 + k\eta_l^2\sigma^2. \end{aligned} \quad (65)$$

That is,

$$\begin{aligned} & \mathbb{E}\|\omega_{t,i,k} - \omega_t\|^2 \\ & \leq \sum_{\tau=0}^{k-1} (8K^2\eta_l^2 L c_{p_B,i} (f(\omega_t) - f(\omega^*)) + 2K^2\eta_l^2 c_{p_G,i} + 2K^2\eta_l^2 (\sum_{\tau=1}^{t-1} p_{\tau,i})^2 R^2 + K\eta_l^2\sigma^2) (4K^2\eta_l^2 L^2 c_{p_B,i})^\tau \end{aligned} \quad (66)$$

$$\leq \frac{8K^2\eta_l^2 L c_{p_B,i} (f(\omega_t) - f(\omega^*)) + 2K^2\eta_l^2 c_{p_G,i} + 2K^2\eta_l^2 (\sum_{\tau=1}^{t-1} p_{\tau,i})^2 R^2 + K\eta_l^2\sigma^2}{1 - 4K^2\eta_l^2 L^2 c_{p_B,i}}. \quad (67)$$

Combine the equation (44), (50), (57), and (67), we get

$$\begin{aligned} & \mathbb{E}\|\omega_t + \Delta\omega_t - \omega^*\|^2 \\ & \leq (1 - \frac{\mu\eta}{2}) \mathbb{E}\|\omega_t - \omega^*\|^2 + (-2\eta + 16\eta^2 L c_{p_B} + \frac{1}{N} \sum_{i=1}^N \frac{16K^2\eta\eta_l^2 L c_{p_B,i} (1 + 4\eta L c_{p_B,i})}{1 - 4K^2\eta_l^2 L^2 c_{p_B,i}}) (f(\omega_t) - f^*) + 2\eta^2 c_{p_G} \\ & \quad + \frac{\eta^2\sigma^2}{NK} + \frac{1}{N} \sum_{i=1}^N \left(2\eta^2 (\sum_{\tau=1}^{t-1} p_{\tau,i})^2 + \frac{4K^2\eta\eta_l^2 L (\sum_{\tau=1}^{t-1} p_{\tau,i})^2 (1 + 4\eta L c_{p_B,i})}{1 - 4K^2\eta_l^2 L^2 c_{p_B,i}} \right) R^2 \\ & \quad + \frac{1}{N} \sum_{i=1}^N \frac{2K\eta\eta_l^2 L (2K c_{p_G,i} + \sigma^2) (1 + 4\eta L c_{p_B,i})}{1 - 4K^2\eta_l^2 L^2 c_{p_B,i}} + \frac{2\eta}{N} \sum_{i=1}^N \sum_{\tau=1}^{t-1} p_{\tau,i} R \|\omega_t - \omega^*\|. \end{aligned} \quad (68)$$

Then we notice that

$$-2\eta + 16\eta^2 L c_{p_B} + \frac{1}{N} \sum_{i=1}^N \frac{16K^2 \eta \eta_l^2 L^2 c_{p_B, i} (1 + 4\eta L c_{p_B, i})}{1 - 4K^2 \eta_l^2 L^2 c_{p_B, i}} \leq 0. \quad (69)$$

Use the fact that $\eta = K\eta_l\eta_g$, and solve above inequality, we notice that if η satisfy

$$\eta \leq \frac{\sqrt{3\eta_g^2 + 4c_{p_B, i}\eta_g^4} - \sqrt{4c_{p_B, i}\eta_g^4}}{6L\sqrt{c_{p_B, i}}}, \quad (70)$$

for any $c_{p_B, i}$, convergence can be promised. Define \hat{c}_{p_B} as the largest $c_{p_B, i}$, let $\eta \leq \frac{\sqrt{3\eta_g^2 + 4\hat{c}_{p_B}\eta_g^4} - \sqrt{4\hat{c}_{p_B}\eta_g^4}}{12L\sqrt{\hat{c}_{p_B}}}$, we have $1 - 4K^2 \eta_l^2 L^2 c_{p_B, i} \geq \frac{33 - 8\eta_g^2 \hat{c}_{p_B} + 4\sqrt{3\eta_g^2 \hat{c}_{p_B} + 4\eta_g^4 \hat{c}_{p_B}^2}}{36}$, and then $\frac{1 + 4\eta L c_{p_B, i}}{1 - 4K^2 \eta_l^2 L^2 c_{p_B, i}} \leq \frac{1}{12} - \frac{7}{33 + \sqrt{3\eta_g^2 \hat{c}_{p_B} + 4\eta_g^4 \hat{c}_{p_B}^2} - 2\eta_g^2 \hat{c}_{p_B}} \leq \frac{1}{12}$. Define $c_{R, i} = (\sum_{\tau=1}^{t-1} p_{\tau, i})^2 R^2$, and $c_R = \frac{1}{N} \sum_{i=1}^N c_{R, i}$. Assume $c_1 = 2c_{p_G} + \frac{\sigma^2}{NK} + 2c_R$, $c_2 = \frac{Lc_{p_G}}{3\eta_g^2} + \frac{L\sigma^2}{6\eta_g^2 K} + \frac{Lc_R}{3\eta_g^2}$, and $c_3 = \frac{2}{N} \sum_{i=1}^N \sum_{\tau=1}^{t-1} p_{\tau, i} R$, inequality (68) become

$$\mathbb{E} \|\omega_t + \Delta\omega_t - \omega^*\|^2 \leq (1 - \frac{\mu\eta}{2}) \mathbb{E} \|\omega_t - \omega^*\|^2 - \eta(f(\omega_t) - f^*) + c_1\eta^2 + c_2\eta^3 + c_3\eta \|\omega_t - \omega^*\|. \quad (71)$$

Move $f(\omega_t) - f^*$ to the left side, we get

$$f(\omega_t) - f(\omega^*) \leq \frac{1}{\eta} (1 - \frac{\mu\eta}{2}) \mathbb{E} \|\omega_t - \omega^*\|^2 - \frac{1}{\eta} \mathbb{E} \|\omega_{t+1} - \omega^*\|^2 + c_1\eta + c_2\eta^2 + \varphi_t. \quad (72)$$

Here φ_t is a constant bounded by $c_3 \|\omega_0 - \omega^*\|$. Because of φ_t , the model cannot converge to an arbitrary ϵ ; instead, it can only converge to the neighborhood of $\epsilon + \varphi$, where φ is the weighted sum of the sequence φ_t . The following parts give the convergence rates when models converge to $\epsilon + \varphi$ for convenience.

B.4.3 WEIGHTS OF ROUNDS.

We can carefully tune the $p_{\tau, i}$ to minimize the noise while speeding up the convergence. Here we give the lemma of the best choice of $p_{\tau, i}$.

Lemma B.4. *On round t , when setting $p_{\tau, i} = \frac{D^2}{tD^2 + (t-1)R^2}$ for any $\tau < t$, and $p_{t, i} = \frac{(t-1)R^2 + D^2}{tD^2 + (t-1)R^2}$, we can minimize c_1 and c_2 to get best convergence.*

Proof. Minimizing c_1 and c_2 is equal to minimize $c_{p_G} + c_R$, that is,

$$\begin{aligned} \min_p \frac{1}{N} \sum_{i=1}^N (1 - p_{t, i})^2 R^2 + G^2 + D^2 \left(\sum_{\tau=1}^t p_{\tau, i}^2 \right), \\ \text{s.t. } \sum_{\tau=1}^t p_{\tau, i} = 1, \forall i = 1, \dots, N. \end{aligned} \quad (73)$$

Solving above optimization problem, we get the results. \square

Using lemma B.4, we have $\min\{c_{p_G} + c_R\} = G^2 + D^2 \left(\frac{D^2 + (t-1)R^2}{tD^2 + (t-1)R^2} \right)$. Notice that the value of c_1 , c_2 , and c_3 are changing over t . We use c_1^t , c_2^t , and c_3^t to represent c_1 , c_2 , and c_3 on round t .

B.4.4 CONVERGENCE RESULTS

Strongly convex functions. By equation (81), when $f_{t, i}(\omega)$ are strongly convex functions, using Lemma A.1, and define $q_t = (1 - \frac{\mu\eta}{2})^{1-t}$, we have

$$f(\omega_F) - f(\omega^*) \leq \mathcal{O} \left(\mu \|\omega_0 - \omega^*\|^2 \exp(-\frac{\mu\eta T}{2}) \right) + \frac{1}{\sum_{t=1}^T q_t} q_t (c_1\eta + c_2\eta^2 + \varphi_t). \quad (74)$$

By Lemma A.6, we have,

$$\begin{aligned}
\frac{1}{\sum_{t=1}^T q_t} \sum_{t=1}^T q_t (c_R + c_{p_G}) &= \frac{1}{\sum_{t=1}^T q_t} \sum_{t=1}^T q_t \left(G^2 + D^2 \left(\frac{D^2 + (t-1)R^2}{tD^2 + (t-1)R^2} \right) \right) \\
&= \frac{1}{\sum_{t=1}^T q_t} \sum_{t=1}^T q_t \left(G^2 + D^2 \left(\frac{R^2}{R^2 + D^2} + \frac{D^4}{(R^2 + D^2)^2} \frac{1}{t - \frac{R^2}{R^2 + D^2}} \right) \right) \\
&= \mathcal{O} \left(G^2 + D^2 \left(\frac{R^2}{R^2 + D^2} + \frac{D^4}{(R^2 + D^2)^2} \frac{\ln T}{T} \right) \right). \tag{75}
\end{aligned}$$

For φ_t , by Lemma B.4, we have,

$$\varphi = \frac{1}{\sum_{t=1}^T q_t} \sum_{t=1}^T q_t \varphi_t \leq \mathcal{O} \left(R \left(\frac{D^2}{D^2 + R^2} - \frac{D^4}{(D^2 + R^2)^2} \frac{\ln T}{T} \right) \|\omega_0 - \omega^*\| \right). \tag{76}$$

Then define $c_1^o = \frac{1}{\sum_{t=1}^T q_t} \sum_{t=1}^T q_t c_1^t$, $c_2^o = \frac{1}{\sum_{t=1}^T q_t} \sum_{t=1}^T q_t c_2^t$, we have,

$$f(\omega_F) - f(\omega^*) - \varphi \leq \mathcal{O} \left(\mu \|\omega_0 - \omega^*\|^2 \exp(-\frac{\mu\eta T}{2}) + c_1^o \eta + c_2^o \eta^2 \right) \tag{77}$$

$$= \mathcal{O} \left(\mu \|\omega_0 - \omega^*\|^2 \exp(-\frac{\mu T}{Lc_O}) + \frac{\sigma^2}{\mu NKT} + \frac{c_A}{\mu T} + \frac{c_B}{\mu T^2} + \frac{c_C}{\mu^2 T^2} + \frac{c_D}{\mu^2 T^3} \right), \tag{78}$$

where $c_O = 1 + A^2 + B^2$, $c_A = G^2 + \frac{D^2 R^2}{R^2 + D^2}$, $c_B = \frac{D^6}{(R^2 + D^2)^2}$, $c_C = \frac{L\sigma^2}{\eta_g^2 K} + \frac{Lc_A}{\eta_g^2}$, $c_D = \frac{Lc_B}{\eta_g^2}$.

General convex functions. When $f_{t,i}(\omega)$ are general convex functions ($\mu = 0$), directly use Lemma A.2 we get,

$$f(\omega_F) - f(\omega^*) - \varphi \leq \mathcal{O} \left(\frac{c_O F}{T} + \sqrt{\frac{\sigma^2 F}{NKT}} + \sqrt{\frac{Fc_A}{T}} + \frac{\sqrt{c_B F}}{T} + \sqrt[3]{\frac{c_C F^2}{T^2}} + \frac{\sqrt[3]{c_D F^2}}{T} \right), \tag{79}$$

where $c_O = 1 + A^2 + B^2$, $c_A = G^2 + \frac{D^2 R^2}{R^2 + D^2}$, $c_B = \frac{D^6}{(R^2 + D^2)^2}$, $c_C = \frac{L\sigma^2}{\eta_g^2 K} + \frac{Lc_A}{\eta_g^2}$, $c_D = \frac{Lc_B}{\eta_g^2}$, and $F = \|\omega_0 - \omega^*\|^2$.

The drift of optimal point. Because of information loss, we can't get the true optimal point when considering previous rounds' information. Instead, the drift can be described as

$$\varphi = c_3^o \|\omega_0 - \omega^*\| = \mathcal{O} \left(R \left(\frac{D^2}{D^2 + R^2} - \frac{D^4}{(D^2 + R^2)^2} \frac{\ln T}{T} \right) \|\omega_0 - \omega^*\| \right). \tag{80}$$

Convergence of FedAvg. Notice that FedAvg is a special case of CFL by setting $p_{t,i} = 1$ on round t . Having this, we derive the one round convergence of FedAvg under our formulation as,

$$f(\omega_t) - f(\omega^*) \leq \frac{1}{\eta} \left(1 - \frac{\mu\eta}{2} \right) \mathbb{E} \|\omega_t - \omega^*\|^2 - \frac{1}{\eta} \mathbb{E} \|\omega_{t+1} - \omega^*\|^2 + c_1 \eta + c_2 \eta^2, \tag{81}$$

where $c_1 = 2(G^2 + D^2) + \frac{\sigma^2}{NK}$, $c_2 = \frac{L(G^2 + D^2)}{3\eta_g^2} + \frac{L\sigma^2}{6\eta_g^2 K}$. Then using Lemma A.1, we get the convergence rate when $f_{t,i}(\omega)$ are μ strongly convex.

$$f(\omega_t) - f(\omega^*) \leq \mathcal{O} \left(\mu \|\omega_0 - \omega^*\|^2 \exp(-\frac{\mu T}{Lc_O}) + \frac{\hat{c}_A}{\mu T} + \frac{\hat{c}_C}{\mu^2 T^2} \right), \tag{82}$$

where $c_O = 1 + A^2 + B^2$, $c_A = G^2 + D^2$, $c_C = \frac{L\sigma^2}{\eta_g^2 K} + \frac{Lc_A}{\eta_g^2}$. Besides, when $f_{t,i}(\omega)$ are general convex, we have,

$$f(\omega_F) - f(\omega^*) \leq \mathcal{O} \left(\frac{c_O F}{T} + \sqrt{\frac{\sigma^2 F}{NKT}} + \sqrt{\frac{Fc_A}{T}} + \sqrt[3]{\frac{c_C F^2}{T^2}} \right), \tag{83}$$

where $c_O = 1 + A^2 + B^2$, $c_A = G^2 + D^2$, $c_C = \frac{L\sigma^2}{\eta_g^2 K} + \frac{Lc_A}{\eta_g^2}$, and $F = \|\omega_0 - \omega^*\|^2$.

B.5 PROOF OF CONVERGENCE RATE FOR NON-CONVEX SETTING

$$\mathbb{E}[f(\omega_{t+1})] \leq \mathbb{E}[f(\omega_t)] + \underbrace{\mathbb{E}[\langle \nabla f(\omega_t), \Delta \omega_t \rangle]}_{A_1} + \frac{L}{2} \underbrace{\mathbb{E}[\|\Delta \omega_t\|^2]}_{A_2} \quad (84)$$

For A_1 part, we have,

$$\begin{aligned} & \mathbb{E}[\langle \nabla f(\omega_t), \Delta \omega_t \rangle] \\ &= \frac{-\eta}{NK} \sum_{i=1}^N \sum_{k=1}^K \mathbb{E}[\langle \nabla f(\omega_t), \nabla \bar{f}_{t,i}(\omega_{t,i,k}) \rangle] \end{aligned} \quad (85)$$

$$= \frac{-\eta}{NK} \sum_{i=1}^N \sum_{k=1}^K \mathbb{E} \left[\langle \nabla f(\omega_t), \sum_{\tau=1}^t p_{\tau,i} \nabla f_{\tau,i}(\omega_{t,i,k}) - \sum_{\tau=1}^{t-1} p_{\tau,i} \Delta_{\tau,i}(\omega_{t,i,k}) \rangle \right] \quad (86)$$

$$\leq \frac{-\eta}{NK} \sum_{i=1}^N \sum_{k=1}^K \mathbb{E} \left[\langle \nabla f(\omega_t), \sum_{\tau=1}^t p_{\tau,i} \nabla f_{\tau,i}(\omega_{t,i,k}) \rangle \right] + \frac{\eta}{2N} \sum_{i=1}^N (1 - p_{t,i}) \left(\mathbb{E}[\|\nabla f(\omega_t)\|^2] + R^2 \right) \quad (87)$$

$$\begin{aligned} &= \frac{\eta}{2NK} \sum_{i=1}^N \sum_{k=1}^K \left(\mathbb{E} \left[\left\| \nabla f(\omega_t) - \sum_{\tau=1}^t p_{\tau,i} \nabla f_{\tau,i}(\omega_{t,i,k}) \right\|^2 \right] - \mathbb{E}[\|\nabla f(\omega_t)\|^2] - \mathbb{E} \left[\left\| \sum_{\tau=1}^t p_{\tau,i} \nabla f_{\tau,i}(\omega_{t,i,k}) \right\|^2 \right] \right) \\ &+ \frac{\eta}{2N} \sum_{i=1}^N (1 - p_{t,i}) \left(\mathbb{E}[\|\nabla f(\omega_t)\|^2] + R^2 \right) \end{aligned} \quad (88)$$

From equation (54) we have

$$\mathbb{E}[\|\Delta \omega_t\|^2] \leq \frac{2\eta^2}{NK} \sum_{i=1}^N \sum_{k=1}^K \left(\mathbb{E} \left[\left\| \sum_{\tau=1}^t p_{\tau,i} \nabla f_{\tau,i}(\omega_{t,i,k}) \right\|^2 \right] + \mathbb{E} \left[\left\| \sum_{\tau=1}^{t-1} p_{\tau,i} \Delta_{\tau,i}(\omega_{t,i,k}) \right\|^2 \right] \right) + \frac{\eta^2 \sigma^2}{NK} \quad (89)$$

Then when $\eta \leq \frac{1}{2L}$, the $\mathbb{E} \left[\left\| \sum_{\tau=1}^t p_{\tau,i} \nabla f_{\tau,i}(\omega_{t,i,k}) \right\|^2 \right]$ term can be ignored, since the coefficient number will less than 0. Then the remaining term in A_2 is $\frac{2\eta^2}{N} \sum_{i=1}^N (1 - p_{t,i})^2 R^2 + \frac{\eta^2 \sigma^2}{NK}$. Then we are willing to consider the $\left\| \nabla f(\omega_t) - \sum_{\tau=1}^t p_{\tau,i} \nabla f_{\tau,i}(\omega_{t,i,k}) \right\|^2$. Then we have

$$\begin{aligned}
& \mathbb{E} \left[\left\| \nabla f(\boldsymbol{\omega}_t) - \sum_{\tau=1}^t p_{\tau,i} \nabla f_{\tau,i}(\boldsymbol{\omega}_{t,i,k}) \right\|^2 \right] \\
&= \mathbb{E} \left[\left\| \nabla f(\boldsymbol{\omega}_t) - \nabla f(\boldsymbol{\omega}_{t,i,k}) + \nabla f(\boldsymbol{\omega}_{t,i,k}) - \sum_{\tau=1}^t p_{\tau,i} \nabla f_{\tau,i}(\boldsymbol{\omega}_{t,i,k}) \right\|^2 \right] \tag{90}
\end{aligned}$$

$$\leq 2\mathbb{E} \left[\left\| \nabla f(\boldsymbol{\omega}_t) - \nabla f(\boldsymbol{\omega}_{t,i,k}) \right\|^2 \right] + 2\mathbb{E} \left[\left\| \nabla f(\boldsymbol{\omega}_{t,i,k}) - \sum_{\tau=1}^t p_{\tau,i} \nabla f_{\tau,i}(\boldsymbol{\omega}_{t,i,k}) \right\|^2 \right] \tag{91}$$

$$\leq 2L^2 \mathbb{E} \left[\left\| \boldsymbol{\omega}_t - \boldsymbol{\omega}_{t,i,k} \right\|^2 \right] + \left(B^2 + A^2 \sum_{\tau=1}^t p_{\tau,i}^2 \right) \mathbb{E} \left[\left\| \nabla f(\boldsymbol{\omega}_{t,i,k}) \right\|^2 \right] + \left(G^2 + D^2 \sum_{\tau=1}^t p_{\tau,i}^2 \right) \tag{92}$$

$$\begin{aligned}
& \leq 2L^2 \mathbb{E} \left[\left\| \boldsymbol{\omega}_t - \boldsymbol{\omega}_{t,i,k} \right\|^2 \right] + 2L^2 \left(B^2 + A^2 \sum_{\tau=1}^t p_{\tau,i}^2 \right) \mathbb{E} \left[\left\| \boldsymbol{\omega}_{t,i,k} - \boldsymbol{\omega}_t \right\|^2 \right] \\
&+ 2 \left(B^2 + A^2 \sum_{\tau=1}^t p_{\tau,i}^2 \right) \mathbb{E} \left[\left\| \nabla f(\boldsymbol{\omega}_t) \right\|^2 \right] + \left(G^2 + D^2 \sum_{\tau=1}^t p_{\tau,i}^2 \right) \tag{93}
\end{aligned}$$

Combine equation (88) and (93) we have

$$\begin{aligned}
& \mathbb{E} [\langle \nabla f(\boldsymbol{\omega}_t), \Delta \boldsymbol{\omega}_t \rangle] \\
& \leq \frac{\eta L^2}{NK} \sum_{i=1}^N \sum_{k=1}^K c_{p_B,i} \mathbb{E} \left[\left\| \boldsymbol{\omega}_{t,i,k} - \boldsymbol{\omega}_t \right\|^2 \right] + \eta (c_{p_B} - 1 - \frac{\sum_{i=1}^N p_{t,i}}{2N}) \mathbb{E} \left[\left\| \nabla f(\boldsymbol{\omega}_t) \right\|^2 \right] \\
&+ \frac{\eta}{2} \left(c_{p_G} + \frac{1}{N} \sum_{i=1}^N (1 - p_{t,i}) R^2 \right) \tag{94}
\end{aligned}$$

Then we have

$$\begin{aligned}
\mathbb{E} [f(\boldsymbol{\omega}_{t+1})] & \leq \mathbb{E} [f(\boldsymbol{\omega}_t)] + \frac{\eta L^2}{NK} \sum_{i=1}^N \sum_{k=1}^K c_{p_B,i} \mathbb{E} \left[\left\| \boldsymbol{\omega}_{t,i,k} - \boldsymbol{\omega}_t \right\|^2 \right] + \eta (c_{p_B} - 1 - \frac{\sum_{i=1}^N p_{t,i}}{2N}) \mathbb{E} \left[\left\| \nabla f(\boldsymbol{\omega}_t) \right\|^2 \right] \\
&+ \frac{\eta}{2} \left(c_{p_G} + \frac{1}{N} \sum_{i=1}^N (1 - p_{t,i}) R^2 \right) + \frac{L\eta^2}{N} \sum_{i=1}^N (1 - p_{t,i})^2 R^2 + \frac{L\eta^2\sigma^2}{2NK} \tag{95}
\end{aligned}$$

Because we know

$$\begin{aligned}
& \mathbb{E} \left\| \boldsymbol{\omega}_{t,i,k} - \boldsymbol{\omega}_t \right\|^2 \\
& \leq 4k^2 \eta_l^2 L^2 c_{p_B,i} \mathbb{E} \left\| \boldsymbol{\omega}_{t,i,k-1} - \boldsymbol{\omega}_t \right\|^2 + 4k^2 \eta_l^2 c_{p_B,i} (\mathbb{E} \left[\left\| \nabla f(\boldsymbol{\omega}_t) \right\|^2 \right]) + 2k^2 \eta_l^2 c_{p_G,i} + 2k^2 \eta_l^2 (\sum_{\tau=1}^{t-1} p_{\tau,i})^2 R^2 + k\eta_l^2 \sigma^2. \tag{96}
\end{aligned}$$

That is,

$$\begin{aligned}
& \mathbb{E} \left\| \boldsymbol{\omega}_{t,i,k} - \boldsymbol{\omega}_t \right\|^2 \\
& \leq \sum_{r=0}^{k-1} \left(4k^2 \eta_l^2 c_{p_B,i} (\mathbb{E} \left[\left\| \nabla f(\boldsymbol{\omega}_t) \right\|^2 \right]) + 2k^2 \eta_l^2 c_{p_G,i} + 2k^2 \eta_l^2 (\sum_{\tau=1}^{t-1} p_{\tau,i})^2 R^2 + k\eta_l^2 \sigma^2 \right) (4k^2 \eta_l^2 L^2 c_{p_B,i})^r \tag{97}
\end{aligned}$$

$$\leq \frac{\left(4k^2 \eta_l^2 c_{p_B,i} (\mathbb{E} \left[\left\| \nabla f(\boldsymbol{\omega}_t) \right\|^2 \right]) + 2k^2 \eta_l^2 c_{p_G,i} + 2k^2 \eta_l^2 (\sum_{\tau=1}^{t-1} p_{\tau,i})^2 R^2 + k\eta_l^2 \sigma^2 \right)}{1 - 4k^2 \eta_l^2 L^2 c_{p_B,i}} \tag{98}$$

Let $8K^2\eta_l^2c_{p_B,i} \leq 1$, we have,

$$\begin{aligned} & \frac{1}{NK} \sum_{i=1}^N \sum_{k=1}^K c_{p_B,i} \mathbb{E} \|\omega_{t,i,k-1} - \omega_t\|^2 \\ & \leq \frac{1}{N} \sum_{i=1}^N c_{p_B,i} \frac{\left(4K^2\eta_l^2c_{p_B,i}(\mathbb{E} [\|\nabla f(\omega_t)\|^2]) + 2K^2\eta_l^2c_{p_G,i} + 2K^2\eta_l^2(\sum_{\tau=1}^{t-1} p_{\tau,i})^2R^2 + K\eta_l^2\sigma^2\right)}{1 - 4K^2\eta_l^2L^2c_{p_B,i}} \end{aligned} \quad (99)$$

$$\leq \frac{1}{N} \sum_{i=1}^N c_{p_B,i} \mathbb{E} [\|\nabla f(\omega_t)\|^2] + \frac{1}{2}c_{p_G,i} + \frac{1}{2}(\sum_{\tau=1}^{t-1} p_{\tau,i})^2R^2 + \frac{\sigma^2}{4K} \quad (100)$$

$$= c_{p_B} \mathbb{E} [\|\nabla f(\omega_t)\|^2] + \frac{1}{2}c_{p_G} + \frac{1}{2N} \sum_{i=1}^N (\sum_{\tau=1}^{t-1} p_{\tau,i})^2R^2 + \frac{\sigma^2}{4K} \quad (101)$$

Then we have

$$\begin{aligned} \mathbb{E} [f(\omega_{t+1})] & \leq \mathbb{E} [f(\omega_t)] + \eta \left((L^2 + 1)c_{p_B} - 1 - \frac{\sum_{i=1}^N p_{t,i}}{2N} \right) \mathbb{E} [\|\nabla f(\omega_t)\|^2] \\ & + \frac{\eta}{2} \left(c_{p_G} + \frac{1}{N} \sum_{i=1}^N (1 - p_{t,i})R^2 \right) + \frac{L\eta^2}{N} \sum_{i=1}^N (1 - p_{t,i})^2R^2 + \frac{L\eta^2\sigma^2}{2NK} \\ & + \eta L^2 \left(\frac{1}{2}c_{p_G} + \frac{1}{2N} \sum_{i=1}^N (\sum_{\tau=1}^{t-1} p_{\tau,i})^2R^2 + \frac{\sigma^2}{4K} \right) \end{aligned} \quad (102)$$

Then we must to choose the value of $p_{t,i}$ for better convergence. Follow the idea that we want to train a better model when convergent, we choose $p_{t,i}$ that can minimize the constant term, which is by solving

$$\begin{aligned} \min_p \quad & G^2 + D^2 \sum_{\tau=1}^t p_{\tau,i}^2 + (\sum_{\tau=1}^{t-1} p_{\tau,1})^2R^2 \\ \text{s.t.} \quad & \sum_{\tau=1}^t p_{\tau,1} = 1 \end{aligned} \quad (103)$$

We get same results as when the objective function is convex, that is, $p_{\tau,i} = \frac{D^2}{tD^2 + (t-1)R^2}$ for any $\tau < t$, and $p_{t,i} = \frac{(t-1)R^2 + D^2}{tD^2 + (t-1)R^2}$, and $\min\{G^2 + D^2 \sum_{\tau=1}^t p_{\tau,i}^2 + (\sum_{\tau=1}^{t-1} p_{\tau,1})^2R^2\} = G^2 + D^2 \left(\frac{D^2 + (t-1)R^2}{tD^2 + (t-1)R^2} \right)$. Then we simplify the equation by using $c_0(t)$, $c_1(t)$, and $c_2(t)$ to denote the constant terms, we have

$$\mathbb{E} [f(\omega_{t+1})] \leq \mathbb{E} [f(\omega_t)] - \eta c_0(t) \mathbb{E} [\|\nabla f(\omega_t)\|^2] + \eta c_1(t) + \eta^2 c_2(t) \quad (104)$$

Then we have

$$\frac{1}{T} \sum_{t=1}^T c_0(t) \mathbb{E} [\|\nabla f(\omega_t)\|^2] \leq \frac{\mathbb{E} [f(\omega_0)] - \mathbb{E} [f(\omega^*)]}{\eta} + \eta \frac{1}{T} \sum_{t=1}^T c_2(t) + \varphi \quad (105)$$

Consider c_0 , because the value of B^2 and A can't be constrained, the algorithm can't converge for very large A and B . Here we first consider when $c_0 < 0$, and use c_m to denote the $\min c_0$. Then let $\eta = \frac{\sqrt{KN}}{\sqrt{TL}}$, we derive the convergence rate as

$$\begin{aligned} \frac{1}{T} \sum_{t=1}^T \mathbb{E} \left[\|\nabla f(\omega_t)\|^2 \right] &= O\left(\frac{L(f_0 - f_*)}{\sqrt{TNK}c_m} + \frac{1}{\sqrt{T}} \left(\frac{\sqrt{KN}}{L} \left(\frac{R^2}{R^2 + D^2} \right)^2 + \frac{\sigma^2}{\sqrt{NK}} \right) \right. \\ &\quad \left. + \frac{\sqrt{KN}}{TL} \frac{D^4}{c_m(R^2 + D^2)^2} + \frac{\sqrt{KN}}{T\sqrt{TL}} \left(\frac{D^4}{(R^2 + D^2)^2} \right)^2 \right) \end{aligned} \quad (106)$$

Then we want to analyse when the algorithm won't converge. When the algorithm won't converge, that means $c_0 \geq 0$. Because $c_0 = (L^2 + 1)c_{p_B} - 1 - \frac{\sum_{i=1}^N p_{t,i}}{2N} = \frac{1}{N} \sum_{i=1}^N (L^2 + 1)(1 + A^2 + B^2 \sum_{\tau=1}^t p_{\tau,i}^2) - 1 - \frac{p_{t,i}}{2}$. Then the value of A^2, B^2, L, p decide if $c_0 \geq 0$. Notice that in FedAvg, $p_{t,i} = 1$, and $c_{0,avg} = (L^2 + 1)(1 + A^2 + B^2) - \frac{3}{2}$, and in CFL, we can setting different p to get better convergence. For example, when B is large, setting $p_{\tau,i} = \frac{1}{t}$, we have $c_0 = (L^2 + 1)(1 + A^2 + \frac{B^2}{t}) - 1 - \frac{1}{2t}$. Thus, we draw the conclusion as Then we have following observations:

- *CFL converge faster than FedAvg by reducing the variance terms.* For $c_0 = \frac{1}{N} \sum_{i=1}^N (L^2 + 1)(1 + A^2 + B^2 \sum_{\tau=1}^t p_{\tau,i}^2) - 1 - \frac{p_{t,i}}{2}$, in FedAvg, we have $p_{t,i} = 1$, then $c_{0,avg} = (L^2 + 1)(1 + A^2 + B^2) - \frac{3}{2}$. However, in CFL, we can adjust p , such as when setting $p_{\tau,i} = \frac{1}{t}$, we have $c_0 = (L^2 + 1)(1 + A^2 + \frac{B^2}{t}) - 1 - \frac{1}{2t}$, then the variance term reduce from B^2 to $\frac{B^2}{t}$.
- *The convergence rate of CFL become better for larger t , since c_{p_B} in c_0 become smaller for larger t .*
- Improve N, K will speed up the convergence by reducing the terms about $f_0 - f_*$ and σ^2 . However, larger N and K will cause larger information loss and round drift (terms with R and D), thus, it should be a trade off in practice.

B.6 THEORETICAL RESULTS

We give the full version of Convergence results as follows.

Theorem B.5 (Convergence rate of CFL methods). *Assume $\{f_{t,i}(\omega)\}$ satisfy Assumption 1–4, the output of Algorithm 1 has expected error smaller than $\epsilon + \varphi$, for $\eta_g = 1$, $\eta_l \leq \frac{\sqrt{3+4(1+B^2+A^2)}-\sqrt{4(1+B^2+A^2)}}{6KL\sqrt{1+B^2+A^2}}$, $p_{\tau,i} = \frac{D^2}{tD^2+(t-1)R^2}$ ($\tau < t$), and $p_{t,i} = \frac{(t-1)R^2+D^2}{tD^2+(t-1)R^2}$ on round t . When $\{f_{t,i}(\omega)\}$ are μ -strongly convex functions, we have,*

$$T = \mathcal{O} \left(\frac{Lc_O}{\mu} + \frac{\sigma^2}{\mu NK\epsilon} + \frac{c_A}{\mu\epsilon} + \sqrt{\frac{c_B}{\mu\epsilon}} + \sqrt{\frac{c_C}{\mu^2\epsilon}} + \sqrt[3]{\frac{c_D}{\mu^2\epsilon}} \right), \quad (107)$$

and when $\{f_{t,i}(\omega)\}$ are general convex functions ($\mu = 0$), we have

$$T = \mathcal{O} \left(\frac{c_O F + \sqrt{c_B F} + \sqrt[3]{c_D F^2}}{\epsilon} + \frac{\sigma^2 F}{NK\epsilon^2} + \frac{c_A F}{\epsilon^2} + \sqrt{\frac{c_C F^2}{\epsilon^3}} \right), \quad (108)$$

and when $\{f_{t,i}(\omega)\}$ are non-convex, setting $\eta = K\eta_g\eta_l = \frac{\sqrt{KN}}{\sqrt{TL}}$, when $\frac{1}{T} \sum_{t=1}^T \mathbb{E} \left[\|\nabla f(\omega_t)\|^2 \right]$ reach ϵ we have

$$T = \mathcal{O} \left(\frac{L^2(f_0 - f_*)^2}{NKc_m^2\epsilon^2} + \frac{1}{\epsilon^2} \left(\frac{\sqrt{KN}c_{R1}^2}{L} + \frac{\sigma^2}{\sqrt{NK}} \right)^2 + \frac{\sqrt{KN}c_{R2}}{c_m\epsilon L} \right), \quad (109)$$

where $c_O = 1 + A^2 + B^2$, $c_A = G^2 + \frac{D^2R^2}{R^2+D^2}$, $c_B = \frac{D^6}{(R^2+D^2)^2}$, $c_C = \frac{L\sigma^2}{\eta_g^2 K} + \frac{Lc_A}{\eta_g^2}$, $c_D = \frac{Lc_B}{\eta_g^2}$, $c_{R1} = \frac{R^2}{R^2+D^2}$, $c_{R2} = \frac{D^4}{(R^2+D^2)^2}$, c_m is a constant related to A, B and R , and $F = \|\omega_0 - \omega^*\|^2$. N is the number of chosen clients in each round, and K is the number of local iterations. We elaborate the choice of $p_{t,i}$ in Appendix B.4.3.

Theorem B.6 (Convergence rate of FedAvg under time-varying scenarios). *Assume $\{f_{t,i}(\omega)\}$ satisfy Assumption 1–4, the output of FedAvg has expected error smaller than ϵ , for $\eta_g = 1$ and $\eta_l \leq \frac{\sqrt{3+4(1+B^2+A^2)}-\sqrt{4(1+B^2+A^2)}}{6KL\sqrt{1+B^2+A^2}}$. When $\{f_{t,i}(\omega)\}$ are μ -strongly convex functions, we have,*

$$T = \mathcal{O} \left(\frac{Lc_O}{\mu} + \frac{\sigma^2}{\mu NK\epsilon} + \frac{c_A}{\mu\epsilon} + \sqrt{\frac{c_C}{\mu^2\epsilon}} \right), \quad (110)$$

Method	SRD				BRD			
	SL-SC	LL-SC	SL-GC	LL-GC	SL-SC	LL-SC	SL-GC	LL-GC
FAVG	0.03	0.08	0.33	0.09	0.02	0.01	0.09	0.02
FPROX	0.04	0.07	0.35	0.09	0.02	0.01	0.26	0.02
CFL	0.2	0.09	0.35	0.09	0.25	0.08	0.3	0.08

Table 7: Best learning rate of different algorithms on noisy quadratic model

and when $\{f_{t,i}(\omega)\}$ are general convex functions ($\mu = 0$), we have

$$T = \mathcal{O} \left(\frac{c_O F}{\epsilon} + \frac{\sigma^2 F}{NK\epsilon^2} + \frac{c_A F}{\epsilon^2} + \sqrt{\frac{c_C F^2}{\epsilon^3}} \right), \quad (111)$$

and when $\{f_{t,i}(\omega)\}$ are non-convex, setting $\eta = K\eta_g\eta_l = \frac{\sqrt{KN}}{\sqrt{TL}}$, when $\frac{1}{T} \sum_{t=1}^T \mathbb{E} [\|\nabla f(\omega_t)\|^2]$ reach ϵ we have

$$T = \mathcal{O} \left(\frac{L^2(f_0 - f_*)^2}{NKc_m^2\epsilon^2} + \frac{1}{\epsilon^2} \left(\frac{\sqrt{KN}}{L} + \frac{\sigma^2}{\sqrt{NK}} \right)^2 \right), \quad (112)$$

where $c_O = 1 + A^2 + B^2$, $c_A = G^2 + D^2$, $c_C = \frac{L\sigma^2}{\eta_g^2 K} + \frac{Lc_A}{\eta_g^2}$, and $F = \|\omega_0 - \omega^*\|^2$. N is the number of chosen clients in each round, and K is the number of local iterations.

C EXPERIMENT DETAILS

C.1 NOISY QUADRATIC MODEL

We use the noisy quadratic model introduced in Zhang et al. (2019) to simulate the assumptions we used in the proof. We use the model $f(\omega) = \omega^T \mathbf{A}\omega + \mathbf{B}^T \omega + \mathbf{C}$, where $\omega \in \mathbb{R}^n$ is the parameter we want to optimize, and $\mathbf{A} \in \mathbb{R}^{n \times n}$, $\mathbf{A} \succeq 0$, $\mathbf{B} \in \mathbb{R}^n$, and $\mathbf{C} \in \mathbb{R}$. We construct \mathbf{A} by firstly constructing a diagonal matrix Λ and then constructing \mathbf{A} by let $\mathbf{A} = \mathbf{U}^T \Lambda \mathbf{U}$, where \mathbf{U} is a unitary matrix. Here we control the eigenvalues of \mathbf{A} to control the convexity of model, that is, $\mu \leq \lambda_{min}(\mathbf{A}) \leq \lambda_{max}(\mathbf{A}) \leq L$. Because Λ and \mathbf{A} have same eigenvalues, it's simple to control the eigenvalues of \mathbf{A} by control the eigenvalues of Λ .

To simulate Assumption 2, 3, we formulate the gradient noise model by

$$g_{t,i}(\omega) = \mathbf{A}\omega + \mathbf{B} + \delta_i + \xi_{t,i} + \nu_{t,i,k}, \quad (113)$$

where δ_i denotes the client drift of client j , $\xi_{t,i}$ denotes the round drift of client j on round i , and $\nu_{t,i,k}$ denotes the noise of gradient of client j on round i , iteration k . All of above drifts and noise are generated from Normal distribution with zero mean and different variance.

In practice, to show if the numerical results match our theoretical results, we tried eight settings: large and small L , large and small round drift, and general and strongly convex conditions. For different types of L , we set $L = 20$ for large L , and $L = 5$ for small L . For convexity, we set $\mu = 1$ for strongly convex, and $\mu = 0$ for general convex. For different round drift, we set $\mathbb{E} \|\xi_{t,i}\|^2 = 100$ for big round drift, and $\mathbb{E} \|\xi_{t,i}\|^2 = 0.01$ for small round drift. Besides, we set fixed variance of δ_i and $\nu_{t,i,k}$ for $\mathbb{E} \|\delta_i\|^2 = 0.01$, and $\mathbb{E} \|\nu_{t,i,k}\|^2 = 0.00001$.

We do the gradient descent by let $\omega_{t,i,k+1} = \omega_{t,i,k} - \eta_l g_{t,i}(\omega_{t,i,k})$, and we use $\|A\omega + B\|$ as loss because for convex functions, when it reaches the global optimal point, we should have $\|A\omega + B\| = 0$, and if it is far away from global optimal, $\|A\omega + B\|$ will be large.

Besides, we show that CFL algorithms can tolerate a larger learning rate here. Table 7 shows the best learning rates for different FL algorithms on noisy quadratic model. In Table 7, we denote small round drift as SRD, big round drift as BRD, small L as SL, large L as LL, strongly convex as SC, and general convex as GC. We show that the best learning rate of CFL is the largest. The difference between CFL methods and other FL baselines becomes large when models are strongly convex or with big round drift.

Figure 2 shows the performance of different algorithms, and CFL outperforms other FL baselines significantly in all settings. Besides, the loss curves of CFL are smoother than FL methods, which implies that CFL can reduce the variance of gradients.

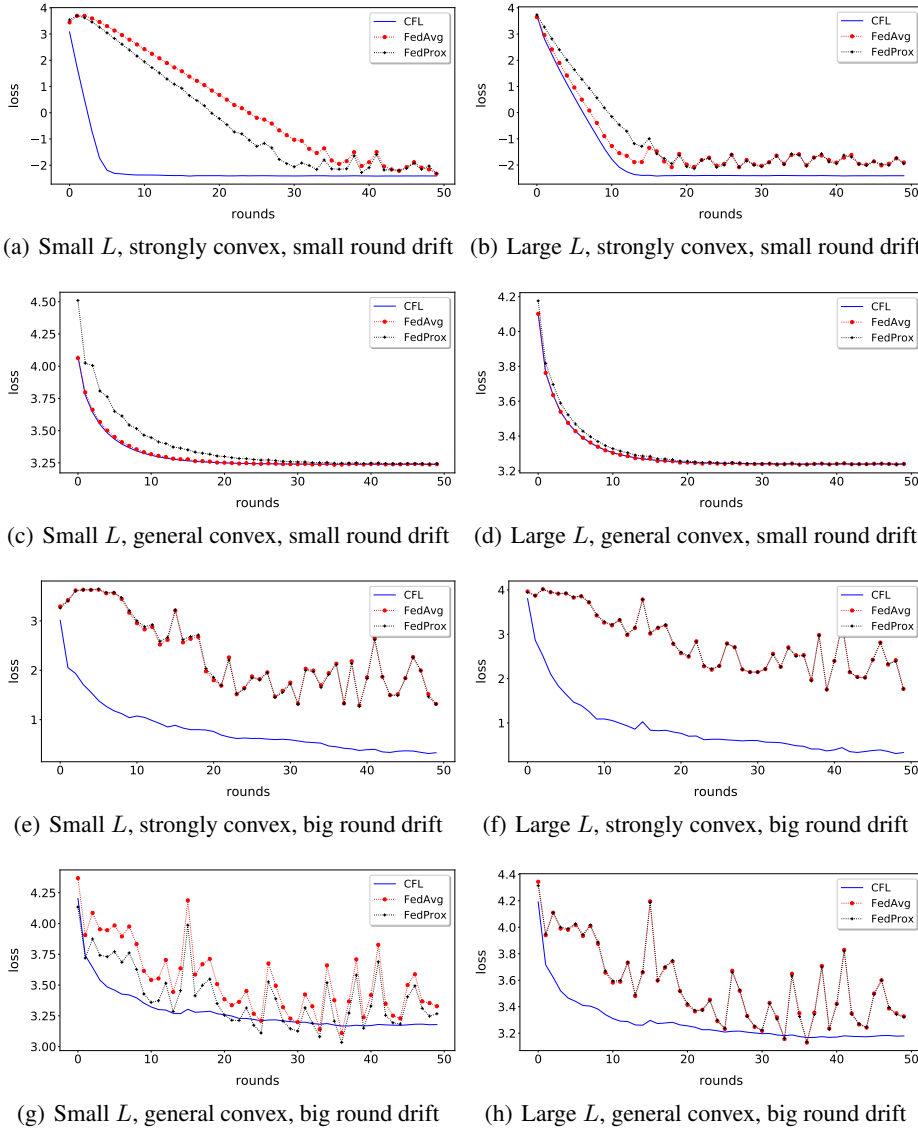


Figure 2: Performance of different algorithms on noisy quadratic model. The curves all evaluate the loss on global test datasets.

C.2 REALISTIC DATASETS

C.2.1 SETUP

We consider federated learning an image classifier on split-CIFAR10 and split-CIFAR100 datasets with ResNet18, and split-Fashion-MNIST dataset with a two-layer MLP. The “split” follows the idea introduced in Yurochkin et al. (2019); Hsu et al. (2019); Reddi et al. (2021), where we leverage the Latent Dirichlet Allocation (LDA) to control the distribution drift with parameter α (See Algorithm 4). Larger α denotes smaller drifts here.

In our experiments, unless specifically mentioned otherwise all datasets are partitioned to 210 subsets for 7 different clients: all clients are selected and trained for 500 communication rounds, and each client samples one of the corresponding 30 subsets randomly for the local training. Note that unless mentioned otherwise the training strategy here applies to all FL baselines and CFL methods, and we evaluate the performance of models on global test datasets. We carefully tuned the hyper-parameters in all algorithms, and we report the results under the optimal settings after many trials. For CFL Regularization, we set the weight of regularization term for $\beta = 1$ on fc layer, and $\beta = 0.1$ for last

block (layer). For FedProx, we set the weight of proximal term $\mu = 0.1$, and for MimeLite, we set the global momentum weight for $\gamma = 0.01$. Besides, for all experiments, we set fixed learning rate $lr = 0.01$. We also naively examined warm-up tuning strategies but can not observe significant improvement on final results.

Construct local datasets with overlap. Follow the partition methods of disjoint local datasets; we first split the whole dataset to $M \times S$ subsets for S different clients: each client has M disjoint local subsets, and we put these M subsets in sequence. For each client, we use a pointer to point to the start position of the current local dataset. Figure 3 show the case when $M = 5$: $D_1 - D_5$ are 5 disjoint local subsets of client i . The pointer point to the start point of a local dataset of the current round and the blue lines bound current subsets. At the beginning of training, pointers belong to each client will point to the beginning of the sequence. At the end of each round, the pointer moves s steps, and if it moves to the end of all the sequence, it will come back to the start point.

In practice, the Cifar10 dataset is partitioned to 210 subsets for 7 clients, and set the size of local dataset $S_l = 285$. Then when we set $s = 285$, the local datasets are disjoint, which means the overlap is 0%. Otherwise, when set $s = 213$, the overlap is 25%, and when set $s = 142$, the overlap is 50%.

C.2.2 APPROXIMATION METHODS

Regularization Methods. We use Taylor Extension to approximate the objective functions of previous rounds, that is,

$$\tilde{f}(\omega) = f(\hat{\omega}) + \nabla f(\hat{\omega})^T(\omega - \hat{\omega}) + \frac{1}{2}(\omega - \hat{\omega})^T \nabla^2 f(\hat{\omega})(\omega - \hat{\omega}), \quad (114)$$

where $\hat{\omega}$ are the parameters of previous rounds. Then the gradient of $\tilde{f}(\omega)$ is,

$$\nabla \tilde{f}(\omega) = \nabla f(\hat{\omega}) + \nabla^2 f(\hat{\omega})(\omega - \hat{\omega}). \quad (115)$$

Having this, we can approximate the gradients of objective functions of previous rounds. The problem is how to approximate $\nabla^2 f(\hat{\omega})$. Here we use two kinds of methods to calculate the Hessian matrices. The first is to use the Fisher Information Matrix as introduced in EWC (Kirkpatrick et al., 2017). The Fisher Information Matrix is equal to the diagonal Hessian matrix when using cross entropy loss functions. The Fisher Information Matrix can be calculated by,

$$F_{ij} = [\nabla f(\hat{\omega})]_{ij}^2, \quad (116)$$

where F_{ij} are the entries of Fisher Information Matrix. Another method is to calculate the diagonal Hessian matrix. We use the PyHessian package (Yao et al., 2020) in this experiment.

In addition, if the parameters or the Hessian matrix changes too much, the performance of this method is constrained. To formulate this problem, assume $\|\nabla^2 f(\omega)\| \leq \epsilon$ for some arbitrary ϵ , we have

$$\|\Delta_{t,i}(\omega)\| \leq \epsilon \|\omega - \hat{\omega}\|^2.$$

The corresponding proof refers to B.3.

In each round, the server will collect Hessian matrices from clients, and store them in a buffer. Then at the beginning of next round, server combine send latest 40 Hessian matrices, gradients, and parameters, and send them to chosen clients. Each clients use these to calculate regularization terms. In practice, we only add regularization terms to the top layers (last block and fc layer of ResNet18). This is based on the assumption that top layers contain more personal information while bottom layers contain more general information. We verified that this strategy perform better than adding regularization terms to all layers in experiments.

Generation Methods. We use MCMC to generate samples in each round. In practice, we initialize \mathbf{x} from uniform distribution, and update \mathbf{x} by,

$$\mathbf{x}^k = \mathbf{x}^{k-1} - \eta \nabla_{\mathbf{x}} E(\mathbf{x}^{k-1}) + \boldsymbol{\omega}, \quad (117)$$

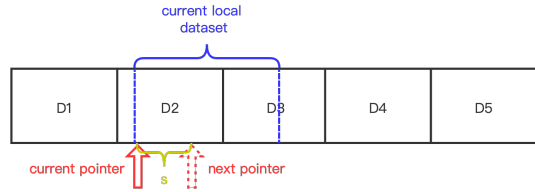


Figure 3: Process of constructing local datasets with overlap. Blue lines bound the current local datasets. Red pointer points to the start of current local dataset.

where $E(\mathbf{x}^k - 1)$ is the function that can measure the distance between \mathbf{x}^{k-1} and the real local distribution. $\omega \sim \mathcal{N}(0, \sigma)$.

In practice, we generate 50-100 samples of each local dataset and add them to the current local datasets for training. However, because of the low quality of the generated data, the improvement is limited. Besides, the generated data will pollute the batch normalization(BN) layer, and we should use real data to refresh BN layer at the end of each round.

Core Set Methods. Another simple yet effective treatment in CL lines in the category of Exemplar Replay (Rebuffi et al., 2017; Castro et al., 2018). This approach stores past core-set samples (a.k.a. exemplars) selectively and periodically, and replays them together with the current local datasets. We tried two sample methods. First is so-called Naive method, in which the samples are uniformly chosen from local datasets. Except of naive select core sets, we also tried another core set sampling method introduced in iCaRL (Rebuffi et al., 2017). See Algorithm 3 for details.

Algorithm 3 iCaRL Construct Core Set

Require: Image set $\mathbf{X} = \{\mathbf{x}_1, \mathbf{x}_2, \mathbf{x}_3, \dots, \mathbf{x}_n\}$ of class y , m : target number of samples, $\phi : \mathcal{X} \rightarrow \mathcal{R}^d$: current feature function

- 1: $\mu \leftarrow \frac{1}{n} \sum_{\mathbf{x} \in \mathbf{X}} \phi(\mathbf{x})$
- 2: **for** $k = 1, \dots, m$ **do**
- 3: $p_k \leftarrow \arg \min_{\mathbf{x} \in \mathbf{X}} \left\| \mu - \frac{1}{k} \left(\phi(\mathbf{x}) + \sum_{j=1}^{k-1} \phi(p_i) \right) \right\|$
- 4: $P \leftarrow (p_1, p_2, \dots, p_m)$

In practice, we save 100 figures of each local dataset and combine them with the current local datasets. Saving core sets perform best compared with these three approximation methods; however, only valid when the number of clients is limited.

C.2.3 ADDITIONAL EXPERIMENTS

Applicability of different algorithms. We list the applicability of different algorithms under various time-varying scenarios in Table 8.

Table 8: The applicability of various algorithms under different time-varying scenarios.

Scenarios	FL baselines				CFL methods	
	FedAvg	FedProx	SCAFFOLD	MimeLite	CFL-Regularization	CFL-Core-Set
Stateful clients	✓	✓	✗	✓	✓	✓
Stateless clients	✓	✓	✗	✓	✓	✗

Convergence curves for different settings. Figure 4 show convergence curves of CFL and FedAvg on different datasets. The settings are the same as results in Table 3. Models are trained on partitioned datasets with $\alpha = 0.1$, and all datasets are partitioned to 210 subsets for 7 clients. To show the difference between different algorithms more clearly, all curves are smoothed by a 1D-Mean-Filter. Results show CFL can converge to a better optimum compare with FedAvg.

Investigating resistance of CFL to time-evolving scenarios. Figure 6 shows the loss curve of CFL-Regularization and FedAvg on different datasets. Models are trained on partitioned datasets with $\alpha = 0.1$, and all datasets are partitioned to 210 subsets for 7 clients. The first column shows the loss curve of the first 300 rounds, and the second column shows the loss of some chosen details. Because of the non-iidness of local datasets, the loss will suddenly rise. Notice that *CFL-Regularization has an apparent mitigation effect on this situation*.

Difference between training and test loss. Figure 5 show the loss on global test data and past appeared training data. We evaluate the model with stateful clients, set $\alpha = 0.2$, and use FedAvg algorithm. We show that *there is no significant difference between loss value on global test data and past appeared training data*.

C.3 ALGORITHMS

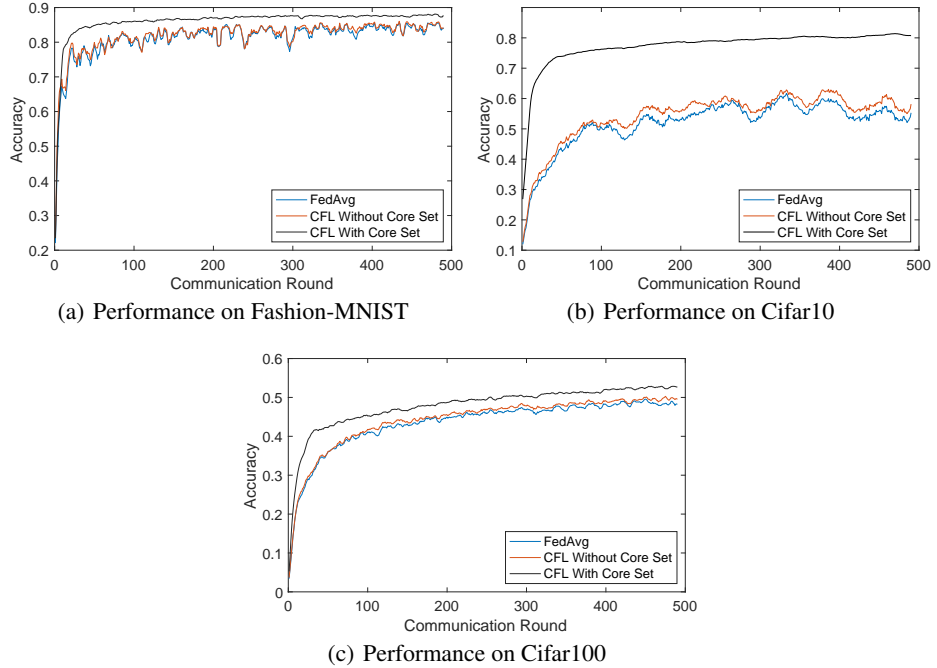


Figure 4: Models are trained on various datasets with $\alpha = 0.1$. CFL Without Core Set method use regularization methods, and CFL With Core Set methods use core set methods. All these two CFL algorithms use FedAvg as backbone.

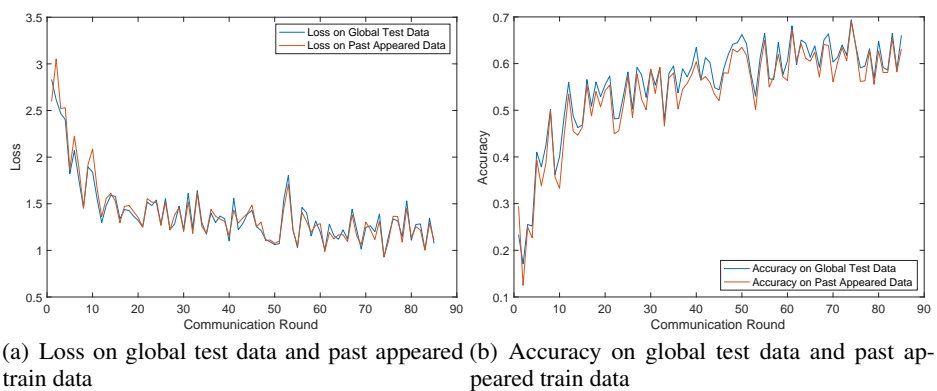


Figure 5: Evaluation on global test data and past appeared training data. We trained ResNet18 on split-Cifar10 dataset with $\alpha = 0.2$ for 85 rounds.

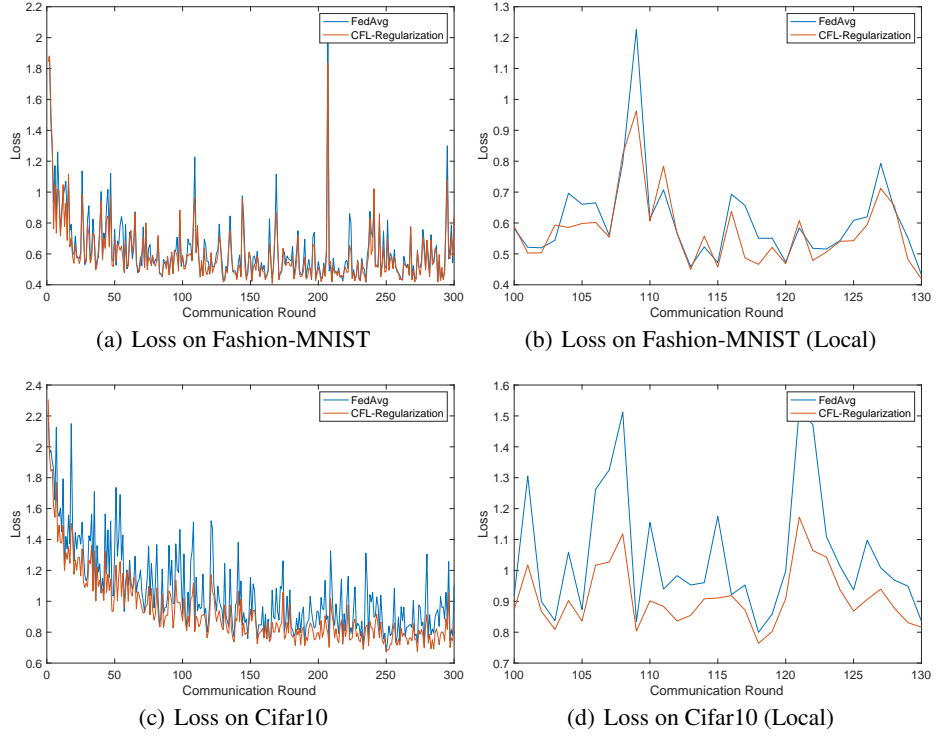


Figure 6: Models are trained on split-Fashion-MNIST and split-Cifar10 datasets with $\alpha = 0.1$. The loss is evaluated on global test datasets. Left column is the full curve of 300 rounds, and figures in right column are partially enlarged curves.

Algorithm 4 Data splitting

Require: S : a list of datasets split by labels, M : the number of clients, N : the size of local datasets, α : the Dirichlet distribution parameter

Ensure: D : split datasets

```

1:  $D \leftarrow []$ 
2:  $G \leftarrow [0, 1, 2, \dots, \text{len}(S)]$ 
3: for  $m = 1, 2, \dots, M$  do
4:    $p = [p_1, p_2, \dots, p_{\text{len}(S)}]$ , where  $p_{t,i}$  denotes the fraction of class  $i$  in total dataset.
5:    $\theta \leftarrow \text{Dirichlet}(\alpha, p)$ 
6:    $D_m \leftarrow \emptyset$ 
7:   while  $\text{len}(D_m) < N$  do
8:      $i \leftarrow \text{multinomial}(\theta, 1)$ 
9:      $y \leftarrow G[i]$ 
10:     $\text{data} \leftarrow \text{uniform}(S[y])$ 
11:     $D_m \leftarrow D_m \cup \{\text{data}\}$ 
12:     $S[y] \leftarrow S[y]/\text{data}$ 
13:    if  $\text{len}(S[y]) == 0$  then
14:       $G \leftarrow G/y$ 
15:       $\theta \leftarrow \text{renormalize}(\theta, i)$ 
16:     $D.append(D_m)$ 

```

Algorithm 5 renormalize

Require: θ : weights for different classes, i : the class that should be deleted

Ensure: θ : renormalized weights

```

1: for  $j = 1, 2, \dots, \text{len}(\theta), j \neq i$  do
2:    $\theta[j] \leftarrow \theta[j]/\text{sum}(\theta)$ 

```

Algorithm 6 SplitdataMain

Require: S : total dataset split by class, T : rounds, K, N, α, β

Ensure: D_{final} : split dataset

```
1:  $D \leftarrow splitData(S, K, N, \alpha)$ 
2:  $D_{final} \leftarrow []$ 
3: for  $i = 1, 2, \dots, K$  do
4:    $S_i \leftarrow splitByClass(D[i])$ 
5:    $N_{local} \leftarrow len(D_m)/T$ 
6:    $D_i \leftarrow splitData(S_i, cluster\_num, N_{local}, \beta)$ 
7:    $D_{final} \leftarrow D_{final} \cup D_i$ 
```
